

N.E. Kornienko¹, A.P. Naumenko¹, L.M. Kulikov²

Observation of Graphite-Like and Diamond-Like Nanostructures in the Raman Spectra of Natural and Synthesized MoS₂ Crystals with Small Carbon Additives

¹Taras Shevchenko National University of Kyiv, Kyiv, Ukraine, nikkorn@univ.kiev.ua, a_naumenko@univ.kiev.ua

²I. Frantsevich Institute for Problems in Materials Science National Academy of Sciences of Ukraine, Kyiv, Ukraine, leonid.kulikov.2402@gmail.com

For the first time, diamond and graphite-like nanostructures in natural molybdenite and synthesized 2H-MoS₂ single crystals were studied using Raman spectroscopy, and a comparative study of carbon nanostructures in synthesized MoS₂ (C) nanocrystallites with carbon 1,0 and 0.5% additives was performed. Detailed numerical analysis of the shape of the observed D and G bands in the spectra at laser excitation $\lambda_L = 632.8$ and 488 nm, including their decomposition into constituent spectral components, allowed to establish the presence of D(k), G(k) components corresponding to the edges of the Brillouin zones, and D(k'), G(k') components, corresponding to the zones middle parts, which indicates the important role of the processes of doubling the size of elementary quasi-cells. Record low frequencies of D lines 1284, 1295 - 1312 cm⁻¹ and high frequencies of G(k) bands at 1387 and 1402 cm⁻¹ were established, that indicate the sizes of diamond- and graphite-like nanostructures less than 1 nm and the narrowing of their phonon quasizones. A new approach has been used to reliably separate close vibrational bands $D \approx G(k)$: as the size decreases and the nanostructures are rearranged, the frequencies D of the bands decrease and the frequencies of the G(k) bands increase. For the first time, a significant effect of 632.8 nm resonant radiation on the formation of MoS₂ + MoO₃ nanocomposite, which activates the formation and ordering of carbon nanostructures, was established. The strengthening of the D bands of the diamond-like nanostructure and the ordering of the graphite-like one with increasing carbon content in MoS₂(C) nanocrystallites have been established. The change of frequencies of D, G and G(k) bands at strengthening of degree of disorder of diamond and graphite-like structures is considered.

Keywords: MoS₂ nanocrystallites, MoS₂ natural single crystals, Carbon additives, Raman spectra, D and G bands structure, graphite-like nanostructures, diamond-like nanostructures.

Received 6 October 2020; Accepted 15 December 2020.

Introduction

The unique physico-chemical properties of inorganic structural analogues of graphene and graphite – transition metal dichalcogenides (TMD) 2H-MX₂ (Me = Mo, W, Ti, Nb, Zr, Ta, Hf, Re; X = S, Se, Te) are determined not only the peculiarities of their two-dimensional structure, but also the presence of the band gap $E_g \sim 1.5 - 2.5$ eV, which is due to their semiconductor properties and the presence of exciton states, which are associated with their resonant properties often manifested in Raman spectra (RS). The properties of TMD can be significantly changed as a result of the transition to the nanocrystalline

state [1]. Recently, much attention has been paid to the development of nanocomposites (hybrid nanomaterials) involving semiconductor 2D graphene-like layers or nanoparticles of d-transition metal dichalcogenides. Physico-chemical properties of nanostructures, and especially nanocomposite materials, are significantly improved, up to unique properties, as a result of the special properties of nanostructures, as well as the impact of synergistic effects compared to those for individual components. Such modern nanomaterials have great prospects for the development of the novel technologies and the creation of new multifunctional devices for various purposes [2, 3]. Therefore, the development of

the modern nanotechnologies for obtaining graphene-like nanostructures and studying their physicochemical properties, including the use of very informative spectral techniques, is of particular importance, which is the basis of this work.

A striking example of the effective use of nanocomposites involving MoS₂ and MoO₃ is their use for catalytic decomposition of water for alternative energy using solar radiation and the resulting hydrogen and oxygen [4, 5]. The photocatalytic activity of the semiconductor catalyst on CdS after its coating only 0.01 wt.% MoS₂ increases 22 times, and at an optimal MoS₂ content of ~ 0.2 wt.% The rate of H₂ increases 36 times, which exceeds the efficiency of precious metals such as Pt, Ru, Au or Pd [4, 5]. Probably, the water adsorbed in MoS₂ nanocomposites with its high-frequency vibrational modes is also an active component of such nanostructures. The developed system of low-frequency vibrations of 2H-MoS₂ ν_1 (E_{1g}) = 278 cm⁻¹, ν_2 (E_{2g}) = 383 cm⁻¹ and ν_3 (A_{1g}) = 408 cm⁻¹, energetically close to the average thermal energy of atom oscillations of kT media, effectively is supplemented by collective vibrational modes of the system of hydrogen bonds of water [6], including higher-frequency libration, deformation and band modes of water. This is the basis for efficient pumping of thermal energy into higher-frequency vibration-exciton (electronic) states due to nonlinear-wave interactions of thermally excited low-frequency vibrational modes. This mechanism can promote not only the catalytic decomposition of water, but also the synthesis of new nanostructures, such as carbon nanostructures with the addition of carbon atoms. The study of the obtained diamond and graphite-like nanostructures in natural and synthesized single crystals, micro- and nanocrystals of MoS₂ with small additions of carbon atoms is the purpose of this article.

Methods for the synthesis of diamond-like structures without the use of high pressure have long been developed and discussed. In particular, in samples of carbon onions (COs) containing 30 - 50 closed fullerene-like shells, under electron irradiation, for example, in an electron microscope, the distances between the carbon shells in COs decrease from 0.36 nm for the outer layers to 0.22 nm for the central parts of CO [7]. According to [8], a pressure of ~ 100 GPa is required for such compression of the inner fullerene-like layers of CO. Due to the huge internal self-compression, COs can play the role of a nanopress for the synthesis of nanodiamonds (ND). In particular, at an electron energy of 1.2 MeV and a dose of > 10²⁴ cm⁻², as well as an increase in temperature to 600 – 1100 K the DA up to 100 nm in size have been obtained [7, 9]. Nanodiamonds are also formed from graphite under high-energy radiation effects [10, 11]. When the fine-grained graphite layer was bombarded with Kr ions (350 MeV, 6 × 10¹² ions/cm² [10]) or Ne ions (3 MeV, 4 × 10¹⁹ ions / cm² [11]), ND of 8 nm and 20 nm were formed. The effect of high-energy laser irradiation on the formation of ND is well demonstrated by irradiating graphite with femtosecond pulses (800 nm, 100 fs) [12].

We observed a significant increase in the intensities of the vibrational bands ν_2 (E_{2g}), ν_3 (A_{1g}) in the Raman spectra (RS) of micro- and nanocrystallites 2H-MoS₂

with laser excitation $\lambda_L = 488$ nm, as well as a strong increase in broadband electronic background (BEB). These effects can be also associated with changes in electronic states, the forces of chemical bonds and internal self-compression. Even greater changes in the properties of MoS₂ nanocrystallites (NCs) were observed by us during the registration of Raman spectra using laser radiation $\lambda_L = 632.8$ nm, that is resonant with exciton states. In this case, together with the manifestation in RS of the properties of stimulated Raman scattering [13] under natural atmospheric conditions, the transformation of the MoS₂ structure into a more complex layered structure of MoO₃ was observed, which will be partially discussed below.

Previously, we studied the occurrence and amplification of BEB in Raman and IR spectra associated with the emergence of new electronic states in the band gap of 2H-MoS₂ crystals ($E_g \approx 2.5$ eV) as a result of strong vibrational-electron interaction (VEI) [14 - 17]. This is consistent with the observed compression up to 5 % of the distance between the layers near the surface of 2H-MoS₂ crystals, as well as a decrease in the distances between metal ions in TMD MX₂ with increasing number of metal group M in the periodic table (IV → V → VI) [18]. There are also distortions of MX₂ TMD structures when M metal atoms are displaced from the centers of structural octahedra. This leads to the appearance of zigzag chains of metal atoms with an abnormally close arrangement. In these chains, electrons that do not participate in MX bonds play an important role in the interactions between metal atoms.

In tetrahedral and octahedral cavities between the X–M–X layers can be intercalated not only carbon atoms C, but also their complexes and even organic molecules. It is important that the interlayer atoms can connect the monolayers X–M–X. In particular, in the nonstoichiometric phases M_{1+Y}X₂, the interlayer chemical bonds with the participation of M atoms differ little from the intralayer bonds MX [18]. As the concentration of Y additives increases, the initial layered structure is transformed into a more densely packed spatial structure. The formation of chains of shorter M–M bonds and the emergence of a spatially coordinated system of chemical bonds can lead to sp³ hybridization for impurity C atoms and the emergence of diamond-like nanostructures within MoS₂ crystallites. In this regard, we have obtained and studied in detail the Raman spectra of both natural and synthesized single crystals of 2H-MoS₂ and natural microcrystals (MC) of molybdenite MoS₂ and synthesized nanocrystallites (NC) of MoS₂(C) with small carbon additives in order to identify the formed internal carbon nanostructures.

I. Experimental part

The method of Raman light scattering is widely used to study the vibrational spectra of TMD MX₂ [19 - 23]. This is due to the fact that the majority of the fundamental vibrations of these compounds are manifested in the Raman spectra. This is facilitated by the low frequencies of the vibrational modes of TMD

Table 1

The results of X-ray studies of nanocrystallites of MoS₂(C)

MoS ₂ (C) Concentration C, wt. %	Unit cell parameters		Unit cell volume nm ³	Crystallographic directions			
	a, nm	c, nm		[013]		[110]	
				reflex. h-w, H _w , rad	average size, nm	reflex. h-w, H _w , rad	average size, nm
0.5	0.3151(2)	1.248(2)	0.1073	0.0422	3.9(2)	0.0188	9.4(6)
1.0	0.3153(2)	1.247(3)	0.1074	0.0422	3.9(2)	0.0194	9.1(6)

MX₂ with the participation of relatively heavy atoms. For the spatial symmetry group D_{6h}⁴ of the crystal structure 2H-MoS₂ for 18 normal vibrational modes the vibrational representation $\Gamma_{\text{vib}} = A_{1g} + 2A_{2u} + 2B_{2g} + B_{1u} + E_{1g} + 2E_{1u} + 2E_{2g} + E_{2u}$ is performed [19]. For 2H-MoS₂ exactly half of the vibrational modes are twice degenerate. Moreover, the vibrations of the crystals 2H-MoS₂ ν_1 (E_{1g}) = 287 cm⁻¹, ν_2 (E_{2g}) = 383 cm⁻¹ and ν_3 (A_{1g}) = 408 cm⁻¹, as well as low-frequency vibration ν_0 (E_{2g}) ≈ 32 cm⁻¹, active in RS.

The vibrations corresponding to the irreducible representations of E_{1u} ~ 379 cm⁻¹ and A_{2u} ~ 457 cm⁻¹ are active in the IR spectra, and the longitudinal and transverse acoustic modes LA, TA, which also belong to the symmetry types A_{2u} and E_{1u}, respectively, in qualitative 2H-crystals MoS₂ does not appear in the IR spectra. Therefore, in the field of basic vibrational modes 2H-MoS₂ the IR spectra are less informative. The frequencies of inactive in the vibrational spectra modes E_{2u} ~ 285 cm⁻¹, B_{1u} ~ 395 cm⁻¹ and B_{2g} ~ 460 cm⁻¹ [24] can be determined by the observed complicated bands or additional bands appearing in the vibrational spectra as a result of the broken of strict selection rules as due to disorientation of the crystal structure, including under the action of more powerful exciting laser radiation. From the given values of frequencies it is seen that the forbidden bands E_{2u} ~ 285 cm⁻¹, B_{1u} ~ 395 cm⁻¹ and B_{2g} ~ 285 cm⁻¹ appear, respectively, near the Raman active bands ν_1 (E_{1g}), ν_2 (E_{2g}) and the overtone of the longitudinal acoustic mode 2LA. But a key role for the purposes of our work is played the fact that the scattering lines of diamond structures in the RS near 1330 cm⁻¹ are characterized by record-high intensities compared to the most intense hydrocarbon lines (benzene, toluene, etc.), which contributes to the detection of diamond- and graphite-like nanostructures at low concentrations of carbon additives.

We studied Raman spectra of synthesized and natural single crystals of layered molybdenum disulfide (2H-MoS₂) with sizes of ~ 2 mm (# 234842 Sigma-Aldrich, 99 %), micron powders of natural molybdenite 2H-MoS₂ (manufactured by Climax Molybdenum Co., USA; CAS 1317-33-5) with an average particle size about 7 μm, as well as synthesized nanocrystallites (NC) with small additions of carbon – MoS₂(C).

According to the high-precision X-ray investigations (full-profile method, use of computer structural

calculations WinCSD [26]), single crystals and microcrystals (MC) 2H-MoS₂, under study are homogeneous, and their crystallographic data and parameters of elementary cells are consistent with literature data [27]: soatial group is P₆3/mm c; a = 0.315956(2) nm, c = 1.22964(2) nm. Data from quantitative chemical analysis correspond to the stoichiometric composition: MoS_{1.99 ± 0.01}.

For the synthesis of MoS (C) nanocomposites the original concept of synthesis of graphene-like 2H-MX₂ (M = Mo, W; X = S, Se) under conditions of low-temperature chemical vapor deposition (CVD) and self-oscillating temperatures was used. Synthesized MoS₂ NCs with a carbon atom content of 0.5 and 1 wt.% have characteristic deviations from the stoichiometric composition (C_xMoS₂: x = 0.067; x = 0.135) and broken chemical bonds at the ends of flat nanoparticles [28]. According to the results of X-ray studies, NC MoS₂(C) have small sizes of ~ 4 and ~ 9 nm in the crystallographic directions [013] and [110], which is shown in Table 1. The estimated number of S–Mo–S monolayers in the z-axis direction n ~ 3. It should be noted that without the addition of carbon atoms NC 2H-MoS₂ reached the size (4 - 5) × 20 (40 - 50) nm and contained 6 - 8 monolayers [29].

It is known that in the Raman spectra of fragments of the "Chelyabinsk" meteorite (2013) with a carbon content of 0.11 % a narrow diamond line with a frequency of 1332 ± 1 cm⁻¹ and a FWHM $\delta\nu = 3.5$ cm⁻¹ was clearly observed [30], that indicates on the prospects of using Raman scattering spectroscopy. Radiation of an Ar⁺ laser with a wavelength of $\lambda_L = 488$ nm (near the electron absorption edge) and a He-Ne laser $\lambda_L = 632.8$ nm (resonant with the exciton states of 2H-MoS₂) were used. During numerical processing of the observed spectra, the optimal numerical smoothing was performed to increase the best signal-to-noise ratio. For a detailed numerical analysis of the structure of the vibrational bands, they were previously allocated to the BEB. When decomposing the selected vibrational bands of carbon nanostructures into constituent spectral components [31, 32], their shape, frequency position, FWHMs and intensities were varied, and the correctness of such decompositions was checked by matching the spectra of the 2-nd derivatives $d^2I/d\nu^2$ from the experimentally observed vibrational bands and calculated ones.

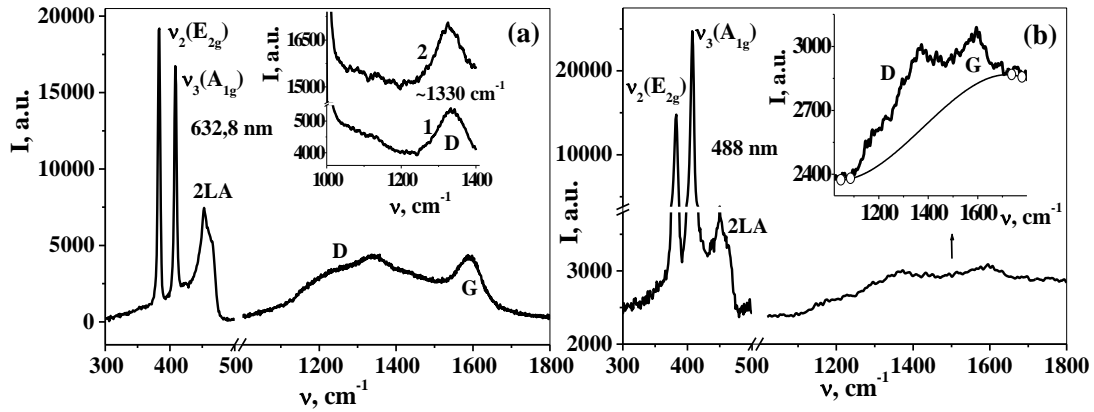


Fig. 1. The comparison of the observed carbon vibrational bands in the high-frequency region and lower-frequency bands in the Raman spectra of natural MoS₂ crystals with sizes of ~ 2 mm and MC with sizes of ~ 7 μm (insert) under excitation of 632.8 nm (a) and synthesized 2H-MoS₂ single crystal under excitation 488 nm (b). The insert shows the selection of vibrational bands of diamond- and graphite-like nanostructures on a broadband background.

II. Observations of diamond- and graphite-like states in Raman spectra of natural and synthesized single crystals of 2H-MoS₂

2.1. General analysis of Raman spectra of 2H-MoS₂ single crystals

Figure 1a shows the Raman spectrum (RS) of natural molybdenite crystals 2H-MoS₂ (# 234842 Sigma-Aldrich) with sizes of ~ 2 mm and in the insert a fragment of RS of natural microcrystals (MC) (Climax Molybdenum Co) with a particle size of ~ 7 μm (spectrum 1) is located. In this case the spectra were excited by resonant radiation of 632.8 nm He-Ne laser. In this spectrum, in addition to the vibrational bands of 2H-MoS₂ ν_2 (E_{2g}) = 383 cm⁻¹, ν_3 (A_{1g}) = 409 cm⁻¹ and the overtone of the longitudinal acoustic mode 2LA ~ 453 cm⁻¹, the wide vibrational bands in the regions of well-known graphite are well manifested. ($G \approx 1580 - 1590$ cm⁻¹) and diamond ($D \approx 1330$ cm⁻¹) bands are well manifested. The exact correspondence of the frequencies of the observed lines ν_2 and ν_3 to the reference value, as well as their small FWHMs $\delta\nu$ indicates the high quality of the studied natural single crystals 2H-MoS₂, although the maximum intensity has the line ν_2 , not ν_3 . Particularly clear diamond D band is manifested in the Raman spectrum of natural MK, which is illustrated by a fragment of the spectrum 1 in the insert Fig. 1a. Observations of the D and G bands of diamond- and graphite-like nanostructures in natural crystals and MC 2H-MoS₂ are associated with the presence of carbon impurities in them.

Figure 1b shows the Raman spectra of the synthesized high-quality single crystal 2H-MoS₂, D and G bands of carbon nanostructures are recognized. In these cases, the bands D and G are associated with the presence in the studied crystals of uncontrolled impurities of carbon, which, of course, more in natural crystals. For more reliable separation of weak bands of overlapping diamond- and graphite-like nanostructures,

the excitation $\lambda_L = 488$ nm was used, which will be discussed in more detail below. In the synthesized single crystal 2H-MoS₂, as usual, the maximum intensity has the line ν_3 (A_{1g}) = 408 cm⁻¹ (see Fig. 1b), although in this spectrum there is a fairly intense BEB. The selection of D and G bands on this background is shown by the insert in Fig. 1b. The BEB was approximated by a cubic polynomial using four basis points, as shown in the insert (2 points on each side of the D and G bands). Note that in natural 2H-MoS₂ single crystals in Fig. 1a the broadband background is virtually absent, which characterizes their good quality.

Thus in natural MC there is a rather strong BEB, the intensity of which is almost three times higher than the intensity of the D band near 1330 cm⁻¹ (see spectrum 1 in the insert Fig. 1a). In the synthesized single crystal 2H-MoS₂ there is an even higher intensity of the BEB, which is approximately seven times higher than the peak intensity of the selected D and G bands (see insert in Fig. 1b). In general, this characterizes the distortion in the structure of the investigated 2H-MoS₂ single crystal and the relatively high quality of natural molybdenite crystals, which allows obtaining graphene-like MoS₂ monolayers from them [33].

Note that for natural 2H-MoS₂ crystals, the maximum intensity of carbon bands is 23.6 % from the peak intensity of the vibrational line ν_2 (E_{2g}) = 383 cm⁻¹, that dominates the Raman spectrum (see Fig. 1a). In the Raman spectra of natural MC, the intensity of D band is 6.2 % from the maximum intensity of the band ν_2 (E_{2g}) = 377 cm⁻¹, which also exceeds the intensity of the shifted line ν_3 (A_{1g}) = 403 cm⁻¹ at excitation $\lambda_L = 632.8$ nm. In the Raman spectrum of the synthesized single crystal at excitation $\lambda_L = 488$ nm, the maximum of the carbon bands allocated on the BEB is only 1.8% from the peak intensity of the line ν_3 (A_{1g}) = 408 cm⁻¹ due to the lower content of carbon impurities. It should be noted that the FWHMs of D and G bands of the studied carbon nanostructures are hundreds of cm, which significantly exceeds the typical FWHM $\delta\nu \approx 2 - 10$ cm⁻¹ of the fundamental lines of diamond and graphite. In the RS of the studied single crystals with increasing excitation power of 632.8 nm, the intensity of the broadband with a

maximum at 463 cm^{-1} in the region of overtone 2LA and inactive vibration $B_{2g} \sim 460\text{ cm}^{-1}$ begins to significantly exceed the intensity of fundamental lines $\nu_{2,3}$.

For comparison, we also studied the Raman spectra of synthesized NC MoS_2 without carbon additives and with carbon additives $\sim 1\text{ wt.}\%$ under excitation at 632.8 nm . A fragment of the spectrum of NC $\text{MoS}_2(\text{C})$ is shown in the insert in Fig. 1a (spectrum 2). For this spectrum, an increase in the BEB more than three times and large variations in intensity have registered. This was caused the large disorder of the structure in comparison with the spectrum 1 of natural MC of MoS_2 . But the main thing is that in spectrum 2 there is also the D band analyzed by us. In the synthesized samples of MoS_2 without carbon additives, this band was completely absent, which is consistent with the evolving ideology.

2.2 Discussion of the results of numerical analysis of the shape of vibrational bands of diamond- and graphite-like nanostructures in the spectrum of natural single crystals 2H-MoS₂

The Raman spectra of natural and synthesized single crystals of 2H-MoS₂, as well as natural microcrystals show in Fig. 1a, b. The observed carbon bands have a rather complex structure, due to the overlap of the vibrational bands of diamond- and graphite-like structures and the fine structure of these bands, due to both abnormally small size and unusual nanostructure of the analyzed formations. Therefore, when they were numerically decomposed into individual spectral components, the minimum allowable number of components was used, which convey the characteristic features of the observed bands. And then a more detailed decomposition of the most interesting fragments of carbon bands into the required number of spectral components was performed.

The results of numerical decomposition of wide overlapping D and G bands in the region of $1000\text{--}1800\text{ cm}^{-1}$ of Raman spectra of natural 2H-MoS₂ single crystals into the minimum possible number of spectral components of the Lorentz form are shown in Fig. 2a. It

is clear that with the use of a larger number of components it is formally possible to achieve a better approximation for the studied experimental band. But the reliability of the used decomposition is confirmed by the good agreement of the second derivatives $d^2I/d\nu^2$ from the experimental and calculated forms of vibrational bands, that is shown in Fig. 2b. Note, that the negative minima in the spectrum of $d^2I/d\nu^2$ correspond to the individual spectral components. From Fig. 2b it is seen that the spectrum of 2-nd derivatives of the observed contour of the vibrational bands allows better identify individual spectral components strongly overlapped. It is important that the 2-nd derivative of the calculated total circuit well reproduces the basic minima of the 2-nd derivative of the experimental spectrum, that characterizes the good quality of decomposition in Fig. 2a.

The main difficulty in the interpreting the selected spectral components is due to the fact that the vibrational states of the diamond structure in the center of the Brillouin zone (BZ) are close to the positions of the vibrational states of graphite at the edges of the BZ.

It is known that when the graphite structure is disordered, for example, by doubling the size of unit cells and the processes of "folding" of phonon curves $\omega(k)$, the states at the edge of the BZ are transformed into the center of the zone and resolved in the vibrational spectra approaching the allowed D bands of diamond-like structure. Since the vibrational states with large wave vectors k are at the edge of the BZ, we will denote the corresponding bands of the graphite structure by $G(k)$. Note, that in many publications on the study of disordered graphite, the band $G(k)$ was denoted by the D band due to their defect-induced nature. In this paper, the bands of diamond-like structure are naturally called D bands, including bands $D(k)$ associated with diamond-like states at the edge of the BZ in the region of large values of k . As a result of the negative dispersion of the phonon branches $\omega(k)$ of graphite- and diamond-like structures ($d\omega/dk < 0$), inequalities for the frequencies of the studied vibrational bands $G(k) < G$ and $D(k) < D$ are

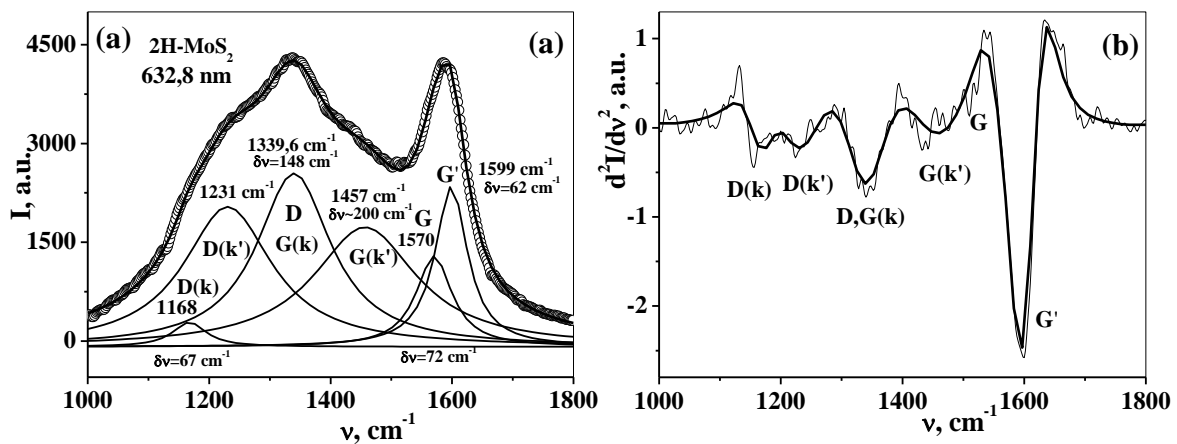


Fig. 2. The results of numerical decomposition of the observed carbon band in the Raman spectrum ($\lambda_L= 632.8\text{ nm}$) of natural crystals of 2H-MoS₂ on the minimum allowable number of individual spectral components of the Lorentz form (a) and comparison of 2-nd derivatives $d^2I/d\nu^2$ from the experimental (thin lines) and calculated forms of vibrational bands (b).

always satisfied. Note that a certain contribution to the observation of G(k) and D(k) bands can make a violation of strict selection rules on the wave vector as a result of defects in the structure and small nanoparticle size, as well as the emergence of new polymorphic modifications of carbon, including the presence clusters containing deformed sp³ bonds [34, 35].

Vibrational D bands of nanodiamonds (ND) are usually situated the range of 1322 - 1326 cm⁻¹ [36], but for abnormally small diamond-like nanostructures in 2H-MoS₂ crystals may have record lower frequencies. Due to the dependence of the frequencies of the G(k) bands in the RS of disordered graphite or the ends of highly oriented pyrolytic graphite (HOPG) on the frequency of laser excitation ν_L , they are characterized by a more significant change in frequency. It is known that as the energy of excitatory laser photons $h_c\nu_L$ increases by 1 eV, the frequencies of G(k) bands of graphite-like structures (including carbon nanotubes) increase by approximately 50 cm⁻¹, and the frequencies of 2G(k) overtones increase by ~ 100 cm⁻¹ [8, 32, 33, 39-41]. In particular, upon excitation at 514.5 nm in the RS from the end of the HOPG single crystal, G(k) bands at 1352 and 1369 cm⁻¹ were observed [37], that allows to clearly distinguish them from D bands of diamond-like structures of the order or less than 1330 cm⁻¹. Similar G(k) bands (1350 - 1352 and 1368 - 1370 cm⁻¹) are observed in MC from the basal planes of disordered HOPG samples implanted with carbon ions at energy of 100 keV and a dose of 10¹⁴ ions/cm² (CHOPG) [38]. However, at laser excitation $\lambda_L = 632.8$ nm, the observed G(k) bands from the edge of graphite 1324 and 1346 cm⁻¹ [37] and from the CHOPG plane 1329 - 1331 cm⁻¹ and 1348 - 1350 cm⁻¹ [38] are partially superimposed on the D band of ND, that complicates their identification.

In this regard, the most intense spectral component 1339.6 cm⁻¹ with a FWHM $\delta\nu = 148$ cm⁻¹ in Fig. 2a for the carbon band in the RS of natural molybdenite at excitation $\lambda_L = 632.8$ nm, we refer to the vibrational D and G(k) overlapping states. In this case, the presence of a diamond-like structure is confirmed by the observation of a fairly intense "shoulder" at 1231 cm⁻¹, which is absent in the nanoporous graphite Raman spectra [42], that will be discussed in more detail below. The presence of a diamond-like phase is confirmed by the presence in the spectrum in Fig. 2a of a narrower component ~ 1168 cm⁻¹ with a FWHM $\delta\nu = 67$ cm⁻¹, that belongs to the D(k) band, corresponding to the edge of the BZ of diamond structure. This is confirmed by the observation in the IR spectrum of detonation ND after annealing at 1000 °C the intense vibrational D(k) band ~ 1160 cm⁻¹ [43 - 45] together with strong bands at 1065 and 1100 cm⁻¹ associated with the inclusion of oxygen atoms in diamond structure [46].

In Fig. 2a, the component at 1231 cm⁻¹ corresponds to the vibrational states in the middle part of the phonon zone of the diamond structure, which is manifested in the RS as a result of repeated doubling of the size of the unit cells and their reflection in the center of the BZ. In what follows, we will denote this spectral component as D(k') (k' ≈ k/2). Our results are confirmed by the observation of similar vibrational D and D(k) bands with frequencies at 1148 and 1239 cm⁻¹ in the Raman spectra of thin CVD

nanocrystalline diamond films with a grain size of 10 - 35 nm [47]. A similar G(k') component close to 1457 cm⁻¹ in Fig. 2a is observed for the graphite-like structure. It should be noted that the G(k') band is approximately halfway between the bands G(k) ~ 1340 cm⁻¹ and G at 1570 cm⁻¹. Two triades of the vibrational components D(k) - D(k') - D and G(k) - G(k') - G of diamond- and graphite-like structures in natural crystals of 2H-MoS₂ are well manifested in the spectrum of 2-nd derivatives d²I/dv² in Fig. 2b. We point out that at excitation $\lambda_L = 632.8$ nm, the negative minima for the spectral components D and G(k) in Fig. 2b actually coincide. The observed triades of spectral components indicate that the appearance of additional vibrational D(k), D(k') and G(k), G(k') bands is mainly due to the processes of disorder of carbon structures associated with the phenomenon of doubling their size unit cells. The model of spatial restriction of phonons in small crystals, including ND with a size of 3 - 10 nm [48] leads only to the displacement of asymmetric vibrational bands in the low-frequency region and their expansion without the occurrence of the considered triple structure. Other mechanisms of formation of bands of diamond structures, which are often considered [34, 35], play a less significant role also.

To separate the D and G(k) bands of diamond- and graphite-like overlapping structures in the region of the maximum of the low-frequency band in Fig. 2a, a more detailed decomposition of this fragment of the Raman spectra into separate spectral components was performed. The obtained results of the decomposition of the maximum of the D ≈ G(k) bands into individual Lorentzians are shown in Fig. 3a. Here, the D component at 1314 cm⁻¹ with a FWHM $\delta\nu = 18$ cm⁻¹, corresponding to a diamond-like nanostructure, is clearly manifested. And the components 1328, 1338 and 1352 cm⁻¹ should belong to the graphite-like structure. All these components G(k) have much smaller FWHM $\delta\nu = 14 - 31$ cm⁻¹ than the bands in Fig. 2a. The good quality of the decomposition of the fragment of the RS of natural crystals 2H-MoS₂ in Fig. 3a is confirmed by the agreement of the 2-nd derivatives d²I/dv² from the experimental and calculated forms of the vibrational bands shown in Fig. 3b. Here, well-defined minima of 2-nd derivatives d²I/dv² correspond to for all spectral D and G(k) components in contrast to Fig. 2b.

Significantly, the selected components of the graphite-like structure at 1328 - 1338 cm⁻¹ and 1352 cm⁻¹ are similar to lines G1(k) and G2(k) with frequencies at 1324 and 1346 cm⁻¹, respectively, in the RS from the edge of the HOPG at the excitation 632.8 nm [37]. The increase in the frequencies of the analyzed components at 1328 and 1352 cm⁻¹ in Fig. 3a on 4 and 6 cm⁻¹ in comparison with the MC from the HOPG edge caused by a decrease in the width of the phonon zones $\omega(k)$ with decreasing of graphite structure, which is manifested primarily in the increase of G1,2(k) frequencies corresponding to the edges of the BZ. The appearance of the additional component at 1338 cm⁻¹ may caused by the existence of even smaller sizes of graphite-like nanostructure or additional folding of the phonon curves $\omega(k)$. It should be noted that the components G1,2(k) at 1328 and 1352 cm⁻¹ highlighted in Fig. 3a are very close

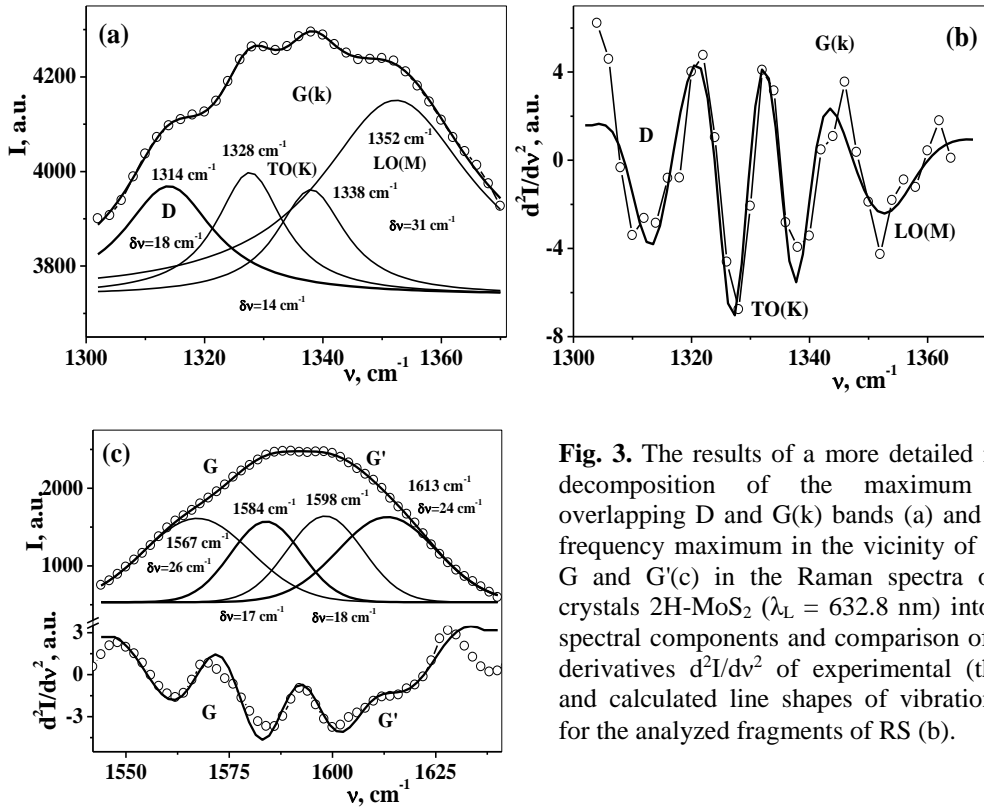


Fig. 3. The results of a more detailed numerical decomposition of the maximum of the overlapping D and G(k) bands (a) and the high-frequency maximum in the vicinity of the bands G and G'(c) in the Raman spectra of natural crystals 2H-MoS₂ ($\lambda_L = 632.8$ nm) into separate spectral components and comparison of the 2-nd derivatives $d^2I/d\nu^2$ of experimental (thin lines) and calculated line shapes of vibrational bands for the analyzed fragments of RS (b).

to similar components in the RS from the CHOPG plane at 1329 - 1331 cm^{-1} and 1348 - 1350 cm^{-1} [38]. This assignment of G1,2(k) bands is confirmed both by the ratio of their intensities (components G1(k) are weaker than G2(k) [38]) and by the close frequency intervals between them ($\Delta\nu \approx 19 - 24 \text{ cm}^{-1}$).

Taking into account the results of the theoretical and experimental studies of the phonon dispersion $\omega(k)$ of different vibrational modes of graphite [49, 50], the observed components G1,2(k) in natural single crystals of 2H-MoS₂ we assign to the transverse and longitudinal optical modes TO (K) and LO (M) at points K and M on the edge of the BZ respectively. This identification of the vibrational bands G1,2(k) is shown in Fig. 3a, b.

In Fig. 2a, close to the component G $\sim 1570 \text{ cm}^{-1}$, the line G' at 1599 cm^{-1} is placed, which corresponds to the maximum frequency in the phonon zone $\omega(k)$ and the maximum density of vibrational states of the graphite structure [49 - 51]. The G' component is more intensive than the G line, which is similar to nanoporous graphite at a certain stage of electrochemical etching [42]. In the IR spectrum of ND annealed at 1000°C, the G' components at 1620 and 1632 cm^{-1} also have a high intensity, and the main component has a frequency of 1597 cm^{-1} [43 - 45]. Note that in Raman spectrum from the HOPG edge at the excitation 632.8 nm, two G' components at 1616 and 1622 cm^{-1} were also observed [37].

The results of more detailed numerical decomposition of the high-frequency maximum in Fig. 2a in the region of the overlapping G and G' bands into individual spectral components are shown in Fig. 3c. It turned out that in this case the best results are given by the decomposition into Gaussian components, which is

associated with inhomogeneous expansion of the spectral components and less deep minima in the spectrum of the 2-nd derivatives $d^2I/d\nu^2$ (see the bottom part of Fig. 3c). Rather good agreement of the 2-nd derivatives $d^2I/d\nu^2$ from the experimental (round symbols) and the calculated shapes of the oscillatory bands confirm the good quality of the decomposition of the G and G' bands into constituent components.

According to Fig. 3c in natural single crystals 2H-MoS₂ a pairs of G and G' components are manifested in spectra. It is important to note that G component at 1567 cm^{-1} corresponds exactly to the position of the G line in the RS of the carbon ion-disordered CHOPG crystal [38, 52]. And the second G component at 1584 cm^{-1} in Fig. 3c should be attributed to a more ordered state of graphite nanowires in natural crystals of 2H-MoS₂. This state of graphite should include the high-frequency G' component at 1613 cm^{-1} , that corresponds to the maximum in the graphite phonon zone $\omega(k)$ inside the BZ. Note that in CHOPG with laser power enhancement from 2 to 100 mW, the frequency of G' line decreased from 1623 to 1606 cm^{-1} [38, 52]. This should also be due to the narrowing of the phonon zones $\omega(k)$ during the desordering action of the laser radiation. The registered frequency at 1613 cm^{-1} (Fig. 3c) of G' component indicates the average degree of disorder of the analyzed graphite-like nanostructure. The spectral components at 1584 and 1613 cm^{-1} , corresponding to the more ordered graphite states, are highlighted in Fig. 3c by thicker lines. Naturally, the second G' component at 1598 cm^{-1} should be attributed to a more disordered graphite-like nanostructure. Thus, we found that in natural crystals of 2H-MoS₂ with sizes up to 2 mm smaller and more disordered graphite-like nanostructures

appear. Moreover, with increasing the degree of disorder, along with a decrease in the frequency of G component the frequency G' line significantly.

As a result of careful analysis of the structure of vibrational bands of diamond- and graphite-like nanostructures formed in natural 2H-MoS₂ single crystals, it was found that by reducing of crystallite size and disordering of structure of these unique nanostructures, the width of the corresponding phonon zones $\omega(k)$ decreases with simultaneous decrease in the frequencies of the D and G bands and an increase in the frequencies of the vibrational D(k) and G(k) bands corresponding to the edges of the BZ. These effects have other clear experimental evidence. In particular, in [53] the frequencies of optical phonons E_{2g} and E_{1u} (1582 and 1590 cm⁻¹) active in Raman and IR spectroscopy decrease by 66 cm⁻¹ when the temperature of graphite increases to 700 K. And in the RS (532 nm) of double-walled carbon nanotubes with increasing temperature up to 2800 °C, the frequency of the G band decreases by 10.5 cm⁻¹, and the frequency of the G(k) band increases by 22.6 cm⁻¹ [54]. Thus, the narrowing of the phonon zones of graphite-like structures is manifested, first of all, in the increase of the lower limiting G(k) frequencies corresponding to the borders of the BZ. The described approach is consistent with the reduction of the D bands frequencies of ND by approximately 10 cm⁻¹ [36]. It should be noted that the laser radiation used to excite the RS can affect the structure of the studied material [55]. In particular, an increase in the radiation power at 514.5 nm from 2 to 100 mW leads to a decrease in the frequency of the G band even in HOPG 1582 → 1578 cm⁻¹ [38, 52]. In this case, in the disordered by implantation of C ions CHOPG the frequency decrease of G band is much greater (1582 → 1567 cm⁻¹), that is exactly equal to the minimum frequency of G band in Fig. 3c.

2.3 Discussion of the results of numerical analysis of the shape of carbon oscillating bands in the Raman spectrum of the synthesized 2H-MoS₂ single crystal

Similar to the numerical analysis of the fine structure of vibrational bands in the Raman spectrum (RS) of natural single crystals 2H-MoS₂, we provided sequentially in two stages the numerical decomposition of carbon bands in the spectrum of the synthesized single crystal 2H-MoS₂. The obtained results in the decomposition of the selected vibrational bands of diamond- and graphite-like nanostructures in the synthesized 2H-MoS₂ single crystal (see the insert in Fig. 1b) into the minimum allowable number of spectral components are shown in Fig. 4a. And the results of a more detailed analysis of the selected fragments of RS at excitation of 488 nm in the region of the vibrational D and D(k) bands are shown in Fig. 4b, c.

Due to the low content of uncontrolled carbon impurities in the synthesized 2H-MoS₂ single crystal in Fig. 4a, the bands D and D(k') have a lower intensity compared to the corresponding bands in Fig. 2a and a more complex structure, which complicates their decomposition into individual spectral components. For simpler separation of the close D and G(k) bands in this case, the excitation of 488 nm was used, at which the band G(k) has a higher frequency and “moves away”

from the D band. Naturally, the band G (k) at a higher energy laser excitation of 488 nm, has a higher frequency of 1365 cm⁻¹ and increased intensity compared to the high-frequency G and G' bands with frequencies of 1560 and 1602 cm⁻¹, respectively.

The presence of a diamond-like structure, as in Fig. 2a, is confirmed by the presence of well-defined low-frequency shoulders close 1175, 1224 and 1289 cm⁻¹, that belong to the D(k), D(k') and D bands (see Fig. 4a). Such shoulders are virtually absent in the RS in disordered samples of pyrolytic graphite, from the edges of graphite crystals, CHOPG or graphite whiskers, where there are only very weak T bands with frequencies of 1072 - 1083 cm⁻¹, as well as bands 810, 867 cm⁻¹ [37, 52, 56, 57], which are significantly shifted in the low-frequency side of the D(k) and D(k') bands considered by us. Spectral bands or shoulders of D(k) and D(k') type are also absent in the RS of nanoporous graphite obtained by electrochemical etching of high-performance single crystals of HOPG [42].

The low-frequency component D(k) at 1175 cm⁻¹ in Fig. 4a, that corresponds to the vibrational states of the diamond-like nanostructure at the border of the BZ, is shifted toward high frequencies compared to the corresponding component at 1168 cm⁻¹ in Fig. 2a. Moreover, the low-frequency wing in Fig. 4a breaks off more sharply in comparison with the long wing in Fig. 2a. This is due to the lower content of carbon impurities and the narrowing of the width of the phonon zone $\omega(k)$ in the synthesized single crystal 2H-MoS₂ compared to the natural analogue. The frequency of D component according to Figs. 3a and 4a decreases (1314 → 1289 cm⁻¹), and the frequency of D(k) component increases (1168 → 1175 cm⁻¹), that is strong evidence of the presence of diamond-like nanostructure. If these components were the longitudinal acoustic modes LA of graphite-like structure, then as the width of their phonon zones decreased, the frequencies of the LA modes would have to decrease. This is confirmed by the data of RS of CHOPG in [37], where the low-frequency T band with increasing energy of exciting photons shifts to the low-frequency side: at excitation $\lambda_L = 632.8$ nm there is a vibrational line at 1115 cm⁻¹, and at $\lambda_L = 488$ nm its frequency decreases to 1072 cm⁻¹, and in less disordered pyrolytic graphite its frequency is 1083 cm⁻¹ [56]. It is clear that the so-called T band [34, 35, 37] in graphite structures should be associated with the LA mode, the frequency of which decreases with the narrowing of the acoustic phonon zone. This further confirms the idea of the narrowing of the phonon zones $\omega(k)$ during the disordering of carbon nanostructures and the weakening of their collective vibrational properties, which we are developing.

In the vicinity of the graphite G band in Fig. 4a, similarly to Fig. 2a, two components G and G' with frequencies 1560 and 1602 cm⁻¹ and comparable FWHM $\delta\nu \approx 60 - 70$ cm⁻¹ are also manifested. Characteristically, here, as in Fig. 2a, the additional component G' has a greater intensity, that characterizes the significant disorder of the structure. Note that in the bulk samples of disordered graphite CHOPG [38, 52], as well as from the edges of HOPG [37] line G' are observed in the range 1616 - 1624 cm⁻¹ and have a much lower intensity

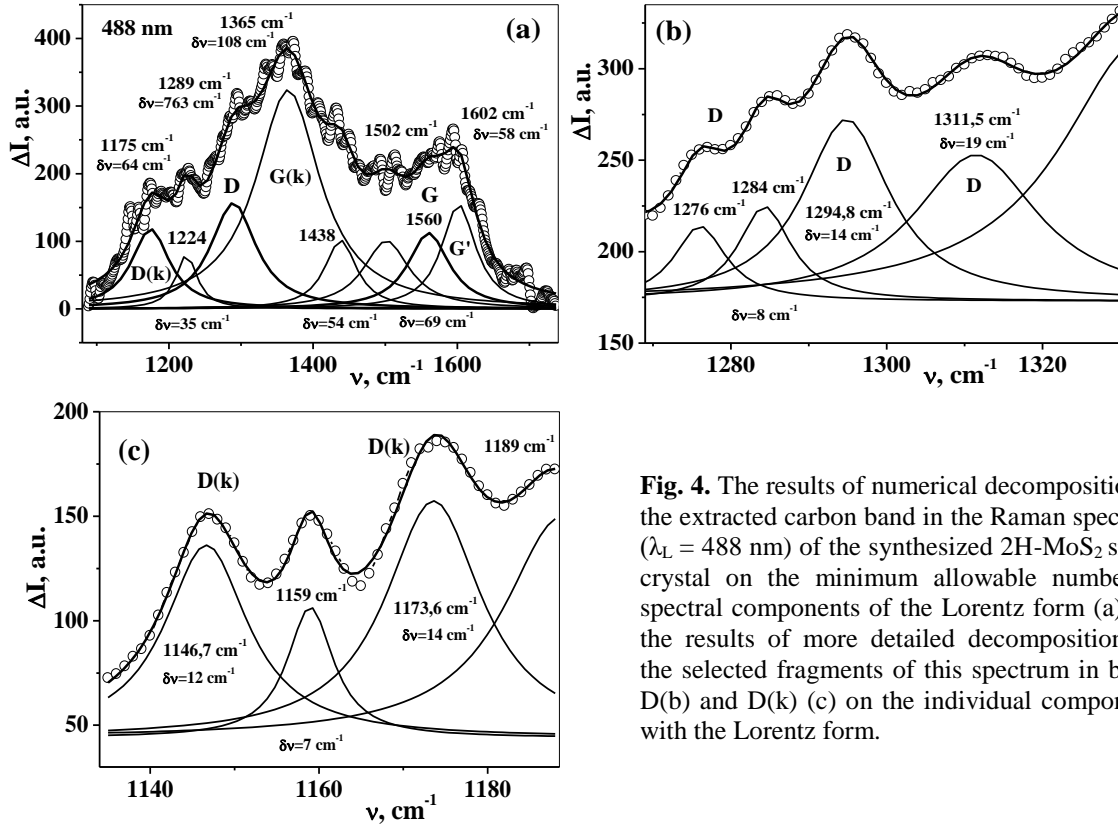


Fig. 4. The results of numerical decomposition of the extracted carbon band in the Raman spectrum ($\lambda_L = 488$ nm) of the synthesized 2H-MoS₂ single crystal on the minimum allowable number of spectral components of the Lorentz form (a) and the results of more detailed decompositions of the selected fragments of this spectrum in bands D(b) and D(k) (c) on the individual components with the Lorentz form.

compared to the main G line 1581 - 1582 cm⁻¹. But with the increasing laser excitation power up to 100 mW and increasing the temperature of the CHOPG ~ 815 K, the frequency of G' components decreases to 1606 cm⁻¹ [38]. Note that in nanoporous graphite, the frequency of the line G' is 1605 cm⁻¹ and its intensity increases sharply [42].

In contrast to the RS in Fig. 2a with one G(k) band at 1457 cm⁻¹, in Fig. 4a there are two less intense G(k') bands with frequencies at 1438 and 1502 cm⁻¹. Their frequencies are on different sides of the component at 1457 cm⁻¹ in natural crystals. As mentioned above, the appearance of the G(k) component at 1365 cm⁻¹, that corresponds to the border of the BZ, is associated with doubling the size of the elementary quasi-cells of graphite-like nanostructures. And the appearance of the G(k') components (approximately in the middle between the lines G(k) and G) is associated with the re-doubling of the size of graphite-like quasi-cells. In the more complex case we are considering, the appearance of two bands of type G(k') at 1438 and 1502 cm⁻¹ can be explained by the repeated tripling of the sizes of elementary quasi-cells, which is associated with a stronger disorder of graphite-like nanostructure in the synthesized 2H-MoS₂ single crystal.

The results of a more detailed numerical decomposition of the selected fragment of the RS in Fig. 4a in the area of diamond-shaped D bands are shown in Fig. 4b. Here on the low-frequency wing of the more intense G(k) band four D components of the Lorentz form with frequencies at 1276, 1284, 1295 and 1312 cm⁻¹

appears. In our opinion, the most intense high-frequency components at 1295 and 1312 cm⁻¹ are associated with diamond-like nanostructures of small size. Note that their frequencies are significantly lower than in detonation ND with sizes of ~ 5nm. And the lower-frequency components at 1276 and 1284 cm⁻¹ can be caused by repeated multiplication of the sizes of elementary quasi-cells in diamond-like nanostructures of smaller sizes, which leads to additional folding of phonon-like curves $\omega(k)$ and manifestation in the vibrational spectra the states inside BZ. This is consistent with a decrease in the FWHMs of the spectral components at 1280 cm⁻¹ ($\delta\nu = 8$ cm⁻¹) compared to the higher-frequency components at 1295 and 1312 cm⁻¹ ($\delta\nu = 14 - 19$ cm⁻¹), due to the larger values of the slope $|dv/dk|$ for phonon-like branches in the middle part of the BZ.

Similarly, the fine structure of the vibrational bands in the region of diamond-like states D(k) near the BZ border is illustrated in Fig. 4c. Here three bands of the Lorentz form with frequencies at 1147, 1159 and 1174 cm⁻¹ are clearly shown. We can assume that the two most intense components at 1147 and 1174 cm⁻¹, as in the region of D lines, belong to the D(k) states near the border of the BZ of diamond-like nanostructures, respectively, with a decrease in their size. A less intense component at 1159 cm⁻¹ is associated with the reflection of the adjacent parts of the phonon-like branches in the center of the BZ as a result of successive multiplication of the sizes of the elementary quasi-cells during the disordering of the diamond-like nanostructure.

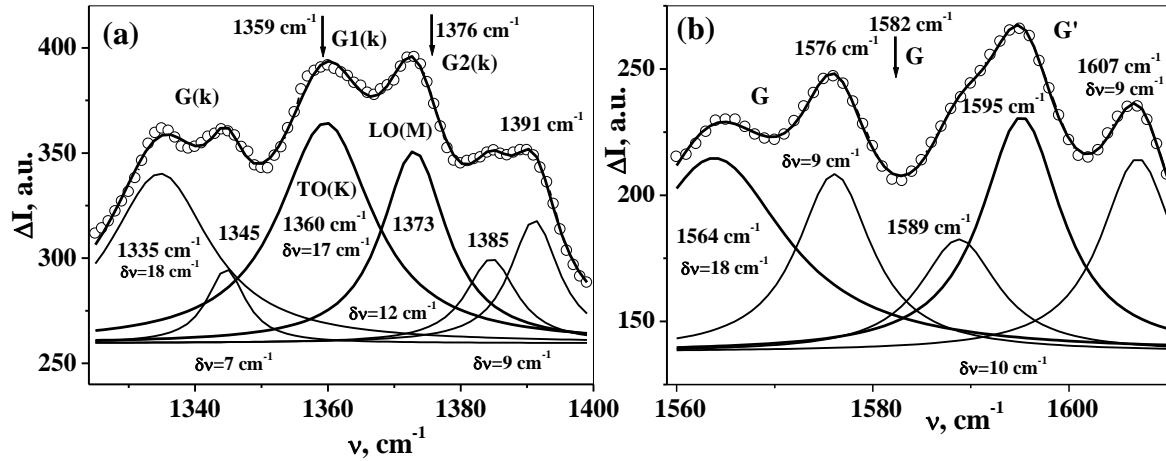


Fig. 5. The results of numerical decomposition of Raman spectra fragments of the synthesized 2H-MoS₂ single crystal ($\lambda_L = 488$ nm) in the region of vibrational G1,2(k) (a) and G, G' (b) bands into individual spectral components of the Lorentz form.

Figures 5a and 5b show the results of a more detailed analysis of RS fragments of the synthesized 2H-MoS₂ single crystal in the regions of intensity maxima (see Fig. 4a) corresponding to the G1,2(k) and G, G' vibrational bands. In the top of Fig. 5a, the arrows indicate the positions of the vibrational bands G1(k) at 1359 cm⁻¹ and G2(k) at 1376 cm⁻¹ in the RS of the ionically disordered CHOPG crystal also at excitation and 488 nm [38]. It is seen that the most intense vibrational lines in Fig. 5a at 1360 and 1373 cm⁻¹ are very close to the components G1,2(k) in CHOPG and naturally must have the same origin. In accordance with the above and Fig. 3a, these components relate to the transverse and longitudinal optical modes TO (K) and LO (M) at points K and M at the borders of the BZ. The higher-frequency components at 1385 and 1391 cm⁻¹ may be due to the re-assembly of the phonon branches $\omega(k)$ of the graphite-like nanostructure as a result of further multiplication of the dimensions of the spatial quasi-cells. This is consistent with a decrease in their FWHMs $\delta\nu = 9$ cm⁻¹ compared with the FWHMs of G1,2(k) components $\delta\nu = 12 - 17$ cm⁻¹. But they can also be associated with abnormally small sizes of graphite-like nanostructures with smaller widths of the corresponding phonon quasizones.

The lower frequency components at 1335 and 1345 cm⁻¹ in Fig. 5a should also refer to the G(k) bands of the graphite-like structure, although their frequencies are lower than the frequencies of the G(k) bands 1357 - 1359 cm⁻¹ in Raman spectrum of pyrolytic graphite and CHOPG [38, 56]. However, the reduction of the frequencies of G(k) in this case to a value 1335 cm⁻¹ may indicate a strong effect of excitation laser radiation on some graphite-like nanostructures. As a result, the chemical bonds C-C became weaker and the frequencies of the G(k) and G bands reduce. This is confirmed by the results of [58], where in the RS of multiwall carbon nanotubes with increasing power of excitation laser radiation 514.5 nm from 0.1 mW to 10 mW, the frequency of G(k) band decreases from 1360 to 1346.5 cm⁻¹, and the the frequency of G band decreases from 1599 to 1577.5 cm⁻¹. Thus, in the studied

carbon nanostructures in the synthesized 2H-MoS₂ single crystal with a slight carbon additives, an even stronger disordering effect of laser radiation $\lambda_L = 488$ nm was actually detected, as a result of which the frequency of G(k) band decreased up to 1335 cm⁻¹. Note that a similar decrease in the frequency of G(k) band was observed in the RS from the edges of the graphite crystal at excitation of 780 nm [37].

Figure 5b shows the results of numerical analysis of vibrational bands of graphite-like nanostructures in the region of their main bands G and G'. In full agreement with the discussion of Fig. 5a, there is a significant shift of the frequencies of G bands at 1564 and 1576 cm⁻¹ towards lower frequencies compared to the reference value of 1582 cm⁻¹ for HOPG and CHOPG [37, 38, 51, 52]. This value is indicated by an arrow in Fig. 5b. The frequencies of G' bands at 1595 and 1607 cm⁻¹ are also shifted to the low-frequency side relative to their position 1616 - 623 cm⁻¹ in the disordered crystals of CHOPG or in the RS from the edges of HOPG [37, 38, 51, 56]. The spectral components at 1564 and 1595 cm⁻¹ should be attributed to a more disordered nanostructure (they are highlighted in Fig. 5b by thicker curves), and a pair of spectral components at 1576 and 1607 cm⁻¹, which are close to the frequencies of G and G' bands with increasing excitation power up to 100 mW [38, 52] attributed to the more ordered nanostructures.

III. Study of diamond-like and graphite-like states in Raman spectra of synthesized nanocrystallites of MoS₂ with small carbon additives

3.1. General analysis of Raman spectra of synthesized MoS₂ nanocrystallites with carbon additives and their structural changes

In connection with the detection of diamond-like

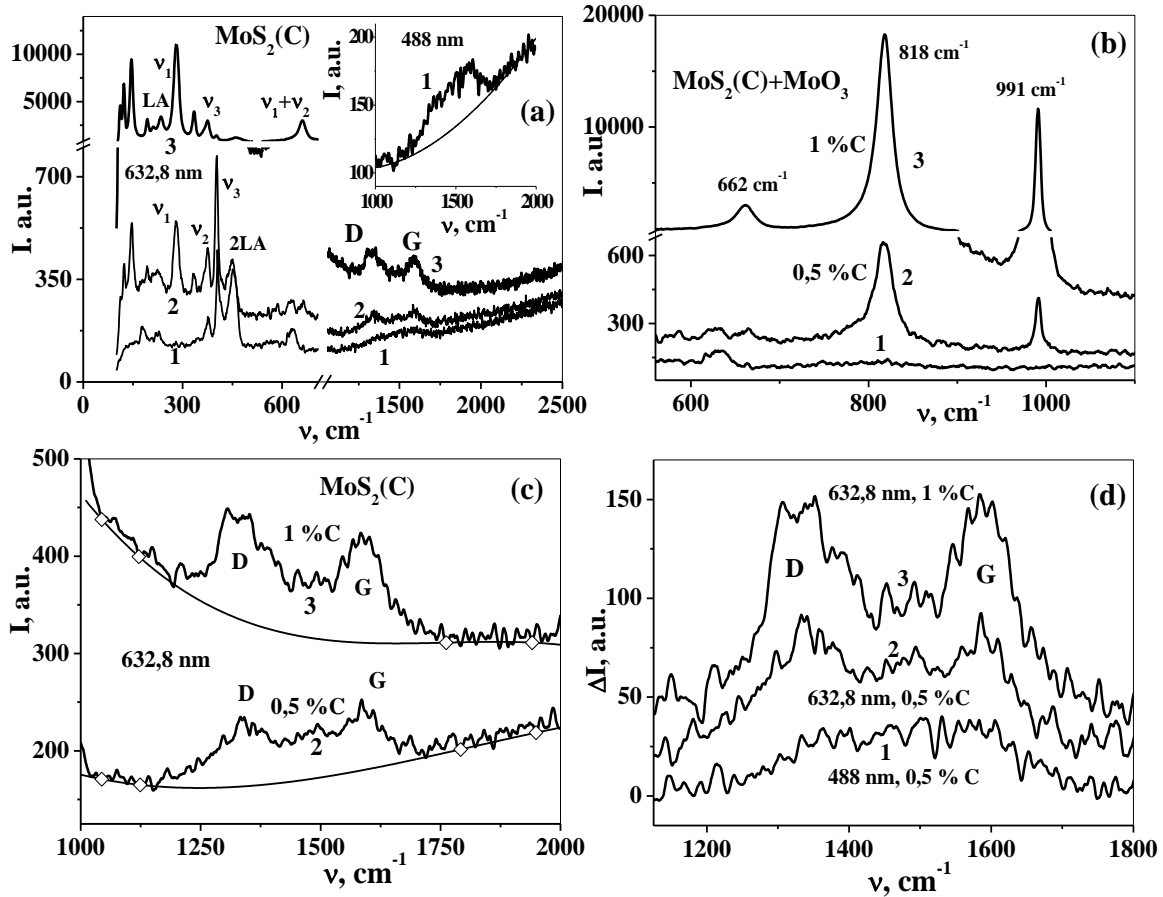


Fig. 6. The comparison of overview RS of MoS₂(C) NC with carbon content of 0.5 wt.% (Spectra 1,2) and 1 wt.% (spectrum 3) at excitation 488 nm (1) and 632,8 nm (2,3), comparison of the fragments of observed RS in the region of the main vibration bands of laser-induced nanostructures α -MoO₃ (b), as well as the allocation of broad carbon bands on a broadband background at excitation 488 nm (insert in Fig.6a) and 632.8 nm (c) and comparison of selected D and G bands of diamond-like and graphite-like nanostructures (d).

inclusions in natural and synthesized single crystals of 2H-MoS₂, natural microcrystals and nanocrystallites (NCs) with carbon additives – MoS₂ C), we provided a more thorough study of Raman spectra (RS) of synthesized NCs with more precise control of carbon additive concentrations. and a detailed numerical analysis of the observed carbon bands. In contrast to our previous publication [59], in this article, in addition to the first study of carbon nanostructures in 2H-MoS₂ single crystals, the fine structure of complex vibrational bands of diamond- and graphite-like nanostructures in synthesized MoS₂(C) NCs with small carbon additives was studied in more detail. In addition to the 632.8 nm He-Ne laser excitation (resonant with exciton states), we also used 488 nm Ar+ laser radiation. The obtained results are partially presented in Fig. 6a. Here is a comparison of the overview RS of MoS₂(C) with a carbon content of 0.5 wt.% (Spectra 1 and 2) and 1 wt.% (Spectrum 3). At 488 nm, a simpler Raman spectrum (spectrum 1) is observed, in which narrow vibrational lines ν_2 (E_{2g}), ν_3 (A_{1g}) and wider overtone bands of longitudinal acoustic vibrations 2LA near 450 cm⁻¹, as well as weak bands of total and difference tones, including with the participation of LA mode at 232 cm⁻¹.

At resonant excitation of 632.8 nm, the RS of MoS₂(C) nanocrystallites are significantly complicated, that is illustrated by spectra 2 and 3 in Fig. 6a. They significantly enhance the BEB, especially strong in the low-frequency region $\nu < 103$ cm⁻¹, where the main vibrational bands of MoS₂, overtones and total tones of the second order of spectra. It should be noted a significant redistribution of the intensities of vibrations ν_1 and ν_3 : the bands ν_1 are significantly enhanced, and the bands ν_3 are abnormally weakened [13]. This indicates a significant change in the properties of NC MoS₂ as a result of the influence of resonant laser radiation of 632.8 nm. This is most pronounced in the amplification of D and G bands – the characteristic for carbon materials in the region of 1200 - 1700 cm⁻¹, which are less intense and with high noise compared with those studied in 2H-MoS₂ single crystals. Significantly, these bands are amplified by changing the excitation wavelength 488 nm \rightarrow 632.8 nm (see spectra 1 and 2) and by increasing the content of carbon additives (0.5 wt.% \rightarrow 1 wt.%; See spectra 2 and 3). We also indicate the growth of the BEB in the high-frequency region of the analyzed spectra, that is also observed in the IR reflection spectra of the MoS₂ NC. This proves the

reliability of the induction of new electronic states in the MoS₂ band gap as a result of strong VEI [14 - 17] and their amplification with increasing carbon content.

Of particular interest is the observation in the RS of MoS₂(C) NC the anomalous amplification of lines 662, 818 and 991 cm⁻¹ under resonant excitation at 632.8 nm and with increasing the content of C atom additives, as illustrated in Fig. 6b. Smaller changes in the MoS₂ Raman spectrum at 632.8 nm excitation pointed by other publications (see, for example, [21]) are associated with the use of larger MoS₂ samples. These lines are very close to the calculated values of the frequencies of the overtone of MoS₂ $2\nu_3 = 816$ cm⁻¹ and the sum tones $\nu_1 + \nu_2 \approx 670$ cm⁻¹, $2\nu_2 + LA = 998$ cm⁻¹. Such differences between the observed and calculated frequencies are quite acceptable taking into account the existing anharmonic frequency shifts, which can be both negative and positive under conditions of strong VEI [14 - 17]. Indeed, in [60], the peak observed in MoS₂ at 820 cm⁻¹ refers to the overtone $2\nu_3$ (A_{1g}), that may be due to the development of forced Raman scattering [13]. This is consistent with a significant increase in the overtone $2A_{1g}$ and the weakening of the main band A_{1g} during ultraviolet excitation of the RS by laser lines 354 nm and 266 nm in the region of strong electron resonance [61].

Interestingly, the strong lines 662, 818 and 991 cm⁻¹ are also associated with the formation of the orthorhombic phase of α -MoO₃, which increases with increasing temperature [23], as well as with increasing power of resonant radiation of 632.8 nm [23, 62, 63]. It was found that at laser power above 1 - 5 mW MoS₂ powders are partially oxidized to molybdenum trioxide MoO₃. Moreover, MoS₂ crystals do not oxidize with the formation of MoO₃ even at high laser power, while the microcrystalline MoS₂ powder is easily oxidized [62]. This is due to the presence in MC and NC a large number of polar edge regions and structural defects available for oxidation. The laser-induced transformation of MoS₂ \rightarrow MoO₃ was also observed during the excitation of RS by 532 nm laser radiation with a power of 3 mW (intensity in the focal region ~ 100 kW/cm²) [63]. It should be noted that α -MoO₃ nanoplates are usually obtained by prolonged heating of MoS₂ nanoshell clusters in air at 350 °C during 5 hours [64].

From Fig. 6b it is seen that at the excitation of 488 nm lines 818 and 991 cm⁻¹ are virtually absent. And for the resonant laser excitation of 632.8 nm there is a partial transformation of MoS₂ \rightarrow MoO₃, that is consistent with the weakening of the lines ν_2 and ν_3 in MoS₂ (spectra 2 and 3). Significantly, this process is enhanced by increasing of carbon content in MoS₂(C) (0.5 % \rightarrow 1 %). This forms large nanoregions of molybdenum trioxide MoO₃, which is confirmed by the strengthening of the lines at 818 and 991 cm⁻¹ in the transition from spectrum 2 to spectrum 3 in 39 and 51 times, respectively (see Fig. 6b). In addition, the FWHM of the main line at 818 cm⁻¹ decreases from the value $\delta\nu = 24.5$ cm⁻¹ to 20.9 cm⁻¹. Note that under the action of continuous laser radiation of 632.8 nm, the conversion of monoclinic *m*-MoO₂ into orthorhombic α -MoO₃ also occurs [65,66]. Moreover, 1D nanorods of MoO₂ are more easily and more strongly oxidized than bulk 3D MoO₂ powder [65]. The nanobranched structure of 1D

MoO₂ nanorods is easily oxidized under the influence of 532 nm laser radiation with a power of 15 mW (diameter 1 μ m). However, an array of similar MoO₂ nanorods of large area and 3D MoO₂ crystals are not oxidized by the laser even at a power of 150 mW for an hour [66], which explains the large scatter of data in the observed RS of NC and MC MoS₂(C). In conclusion, we note that the reverse conversion of thin layers of MoO₃ into nanoplates 2H-MoS₂ was carried out by sulfurization of MoO₃ at a temperature of 650 – 1000 °C in the presence of sulfur vapor [67, 68].

Importantly, both MoS₂ [4, 5, 60, 69 - 71] and MoO₃ [72, 73] exhibit excellent catalytic properties and great potential for photocatalytic fission of water and hydrogen production in solar energy, as well as decomposition of various organic pollutants. For the purposes of hydrogen energy, a composite with a MoO₃ core and a MoS₂ shell is promising [74]. Of particular interest is observed by us the partial transformation of MoS₂ \rightarrow MoO₃ induced by low-power laser radiation of 632.8 nm. Finally, it should be noted that photothermal therapies using MoS₂ and MoO₃ nanostructures provide a powerful new alternative treatment for lung and breast cancer [75, 76].

Zr-doped MoS₂ nanosheets showed excellent catalytic and antibacterial activity compared to undoped MoS₂ [60]. Significant amplification of D and G bands with a higher content of carbon additives in NC of MoS₂ (C = 1 %) (see spectra 2 and 3 in Fig. 6a) and changes in structure under the action of resonant radiation of 632.8 nm indicates an increase in the activity of MoS₂ nanostructure (C) to the formation of graphene-like and diamond-like nanostructures. We attribute this to the increase in wave nonlinearity, which promotes the nonlinear interaction of thermally excited low-frequency vibrational modes with the generation of higher vibrational states. The latter approach the exciton and electronic states, which leads to the amplification of strong VEI, changes in these states and the induction of new electronic states [14 - 17]. In this regard, a special role belongs to the emerging heterostructure of MoS₂-MoO₃. This is due to both the significant enrichment of the spectrum of vibrations in the RS of α -MoO₃ in the region $\nu < 280$ cm⁻¹ [23, 62, 63], and the manifestation here the acoustic vibrational modes of NC MoS₂(C) as a result of the regulating action of radiation 632.8 nm, caused by the coagulation of phonon zones due to the complexity of the spectra in the field of optical modes, that was considered in the previous section. The enriched low-frequency spectrum (see spectra 2 and 3 in Fig. 6a), as well as the vibration resonances of MoO₃ in the region of 600 - 1000 cm⁻¹ (see Fig. 6b) and the higher-frequency D and G carbon bands contribute to the conversion of thermal energy into high-frequency region and the manifestation of the effects of strong VEI [14 - 17].

For a more detailed numerical analysis of the observed D and G bands, they were decomposed on the BEB, that is illustrated by the insert in Fig. 6a for the case of 488 nm excitation and in Fig. 6c for the case of excitation by 632.8 nm radiation. The BEB sections in the region of the analyzed D and G bands, as in Fig. 1b, were approximated by polynomials of the 3-rd degree using two reference points on the low- and high-frequency sides of the selected bands, as shown in Fig.

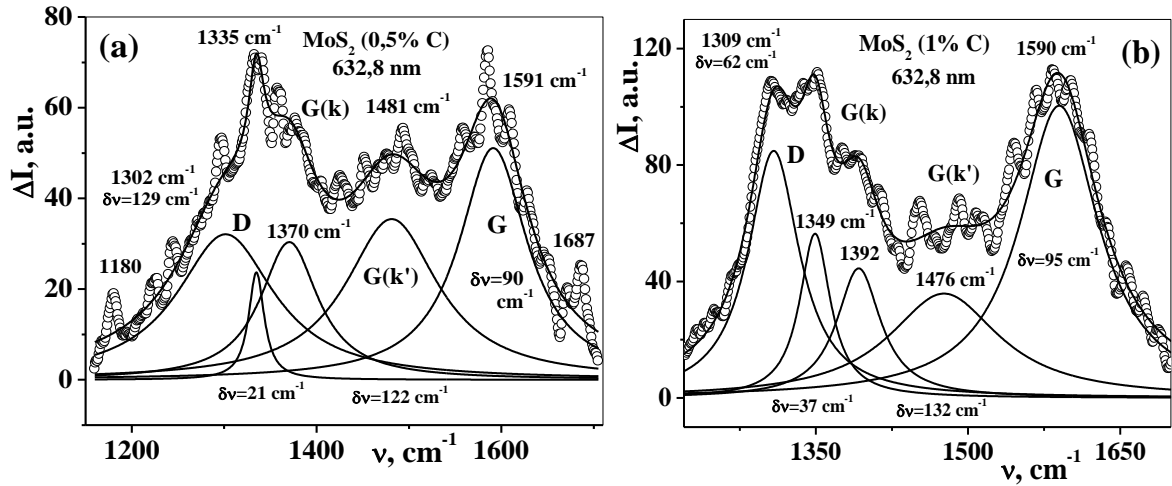


Fig. 7. The results of numerical decomposition of the selected in the Raman spectra of MoS₂(C) NC ($\lambda_L = 632.8$ nm) vibrational D and G bands of diamond-like and graphite-like nanostructures at a carbon content of 0.5 wt.% (A) and 1 wt.% (B) on spectral components of the Lorentz form.

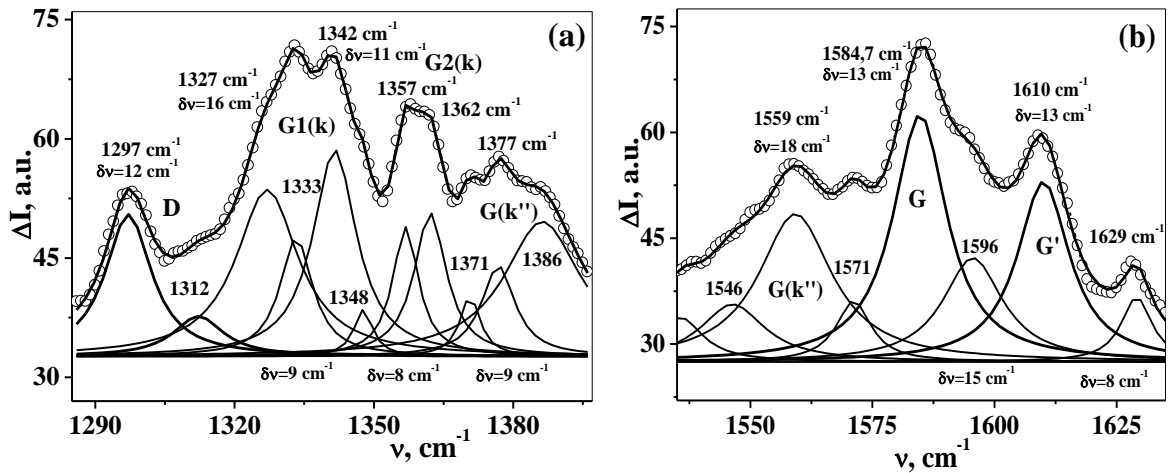


Fig. 8. The results of detailed numerical decomposition of the Raman spectra fragments ($\lambda_L = 632.8$ nm) for NC MoS₂(C) at a carbon content of 0.5 wt.% in the region of diamond D bands (a) and graphite G bands (b) on the spectral components of the Lorentz form.

6c. Comparison of the selected D and G vibrational bands in the three spectra considered by us is shown in Fig. 6d, where for better separation the bands 2 and 3 are shifted up by 20 and 40 a.u. It is seen that in all cases the intensities of the D and G bands are approximately equal to each other. The intensities of the D and G bands for NC MoS₂(C) with a concentration of C = 0.5 wt.% and the excitation change of 488 nm → 632.8 nm (see bands 1 and 2), that additionally shows a significant structure-forming role of the continuous laser radiation used in RS registration. Upon excitation of 632.8 nm and an increase in the concentration of carbon content in the NC MoS₂(C) from 0.5 % to 1 wt.% the intensity of the D and G bands increase more than 1.5 times (see bands 2 and 3).

3.2 Discussion of the results of numerical analysis of the shape of diamond and graphite-like vibrational bands in the Raman spectra of synthesized MoS₂(C) nanocrystals

Numerical decomposition of D and G Raman bands

of synthesized MoS₂(C) into individual spectral components was performed. Due to the fact that the selected vibrational bands in Fig. 6d are characterized by excessive variations in intensity and a more complex structure, we still performed their numerical decomposition into individual spectral components in two stages. Initially, they were decomposed into the minimum allowable number of spectral components, which on average reflect the characteristic structure of these bands. And then in addition the overlapping D, G(k) and G,G' bands were analyzed in more detail taking into account their complex structure.

In both cases, as in Fig. 2a, 3a, 4a, b, c and 5a, b good results gives the decomposition into individual components of the Lorentz form, which well reflect the rather intense distant wings of the analyzed bands. The obtained results for D and G carbon bands in Raman spectra of NC MoS₂(C) at excitation of 632.8 nm and carbon concentrations of 0.5 and 1 wt% when decomposed into a small number of generalized spectral components are shown in Fig. 7a, b. A more detailed

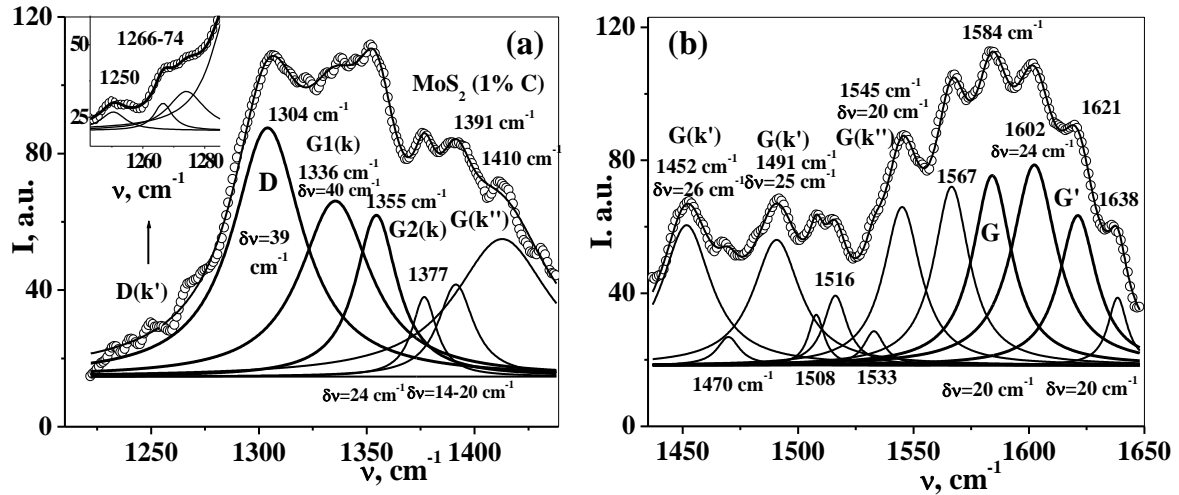


Fig. 9. The results of detailed numerical decomposition of Raman spectrum fragments ($\lambda_L = 632.8$ nm) of NC MoS₂(C) at a carbon content of 1 wt.% In the region of diamond D bands (a) and graphite G bands (b) on the spectral components of the Lorentz form.

decomposition of the selected fragments of the vibrational bands D, G(k) and G, G' at C = 0.5 wt.% are presented in Fig. 8a, b, and in the case of C = 1 wt.% – in Fig. 9a, b. The frequency positions and spectral FWHM $\delta\nu$ of the components are shown in these figures.

The high-frequency spectral bands G at approximately 1590 cm⁻¹ in Fig. 7a, b belong to graphite-like carbon nanostructures. With increasing content of carbon additives in NC MoS₂(C) from 0.5 to 1 wt.% the intensity of the G bands increase approximately twice, as expected. Their large FWHMs ($\delta\nu \approx 90 - 95$ cm⁻¹) are due to their small size and large disorder of graphite-like nanostructures. According to the data of [77], this value of $\delta\nu$ corresponds to the size of nanostructures ~ 1 nm. The lower-frequency bands G(k) at 1370 cm⁻¹ in Fig. 7a and 1349 and 1392 cm⁻¹ in Fig. 7b correspond to the vibrational modes of the graphite-like nanostructure at the edge of the BZ, that are manifested in the vibrational spectra when doubling the size of the elementary quasi-cells of nanographite, which will consist of 8 carbon atoms instead of 4 C atoms.

In Fig. 7a between G(k) and G bands the additional band at 1481 cm⁻¹ with a FWHM $\delta\nu \approx 120$ cm⁻¹ is well shown. Its position well corresponds to the frequency of TO mode in the middle point of the BZ according to the studied phonon dispersion of graphene and graphite [49, 50]. This region of BZ is transformed into the center of the zone during the formation of the lattice by redoubling the size of the elementary quasi-cells of nanographite, and as in Fig. 2a denotes G(k'), where $k' \approx k/2$. With increasing of carbon concentration in the NC MoS₂(C) to 1 wt.%, together with an increase in the intensity of the G bands approximately twice, markedly increase the intensity of the bands G(k) (compare Fig. 7a, b). However, the intensity of the middle band G(k') practically does not change, and its contribution to the spectrum in Fig. 7b is significantly reduced, due to the ordering of the graphite-like structure at a higher content of carbon additives. It should be noted that along with the transformation into the center of the BZ of the middle state of the TO mode (k'), a similar transformation occurs

for the middle state of the LO mode (k'). However, the frequency of LO(k') mode according to the data [49, 50] is ~ 1595 cm⁻¹ and its reflection to the center of the BZ leads to a shift of the G band towards high frequencies and its expansion, that is observed in Fig. 7a, b. It should be noted that when disorganizing the structure and violating of the selection rules the IR active mode $E_{1u} \approx 1588$ cm⁻¹ [51] can contribute to the observed G band too.

The spectral lines at 1302 and 1309 cm⁻¹ in Fig. 7a, b correspond to the D lines of nanodiamonds (ND). The increase in the intensity of the D band more than twice, as well as a decrease in its FWHM $\delta\nu$ from 129 cm⁻¹ to 62 cm⁻¹, ie approximately twice, with increasing content of C atoms in NC MoS₂(C) 0.5 \rightarrow 1 wt.%, due to the increase in size and ordering of the diamond-like nanostructure. At the same time, the sharp component 1335 cm⁻¹ in Fig. 7a at excitation of 632.8 nm in full agreement with components 1328 and 1338 cm⁻¹ in Fig. 3a in the RS of natural 2H-MoS₂ single crystals should correspond to graphite-like states.

In Fig. 7a similarly to the component at 1687 cm⁻¹ on the high-frequency wing of G band, on the low-frequency wing of D band shows a sharp component at 1180 cm⁻¹. Previously, this component was associated with sp³ hybridization, although a deep understanding of this phenomenon was lacking and this band was designated the T band [34, 35]. According to the analysis performed in section 3 (see Fig. 2a and 4a), it is natural to identify the line at 1180 cm⁻¹ with the state D(k). This component in comparison with the bands at 1168 and 1178 cm⁻¹ detected in 2H-MoS₂ single crystals indicates a further narrowing of the phonon zones $\omega(k)$ of the diamond-like structure in MoS₂(C) NC.

In Fig. 8a, b the results of detailed numerical decomposition of the fragments of the Raman spectra of NC MoS₂(C) in the region of D and G bands at a carbon content of 0.5 wt.% and excitation 632.8 nm are presented. The bands D of the diamond-like structure in Fig. 8a include components 1297 and 1312 cm⁻¹, and the components 1327 - 1342 cm⁻¹ undoubtedly belong to the components of the band G1(k) of the graphite-like

structure corresponding to the states TO(K) at point K on the BZ border. And close components 1357 and 1362 cm^{-1} belong to the band G2(k), that corresponds to the states LO(M) near the point M of BZ, as shown above. This structure of the vibrational bands G1,2(k) may be due to the heterogeneity of the studied samples of agglomerates of synthesized NC MoS₂(C). It should be noted that the diamond-like components at 1297 and 1312 cm^{-1} are very close to lines at 1295 and 1312 cm^{-1} in RS of synthesized single crystal 2H-MoS₂ (see Fig. 4b). The appearance of high-frequency components at 1377 and 1386 cm^{-1} in Fig. 8a is associated with a stronger disordering of the graphite-like nanostructure of the NC MoS₂(C) as a result of further multiplication of the sizes of quasi-cells. We will denote such spectral components by G(k'').

Figure 8b shows clear lines G and G' with frequencies of 1585 and 1610 cm^{-1} and FWHM $\delta\nu = 13 \text{ cm}^{-1}$, that characterizes a fairly high quality of graphite-like formations. There are also additional components at 1596 and 1629 cm^{-1} , which are associated with the inhomogeneity of the nanostructure. Similarly to the band G(k'') in Fig. 8a on the low-frequency side of the band G in Fig. 8b, similar components at 1546 – 1559 cm^{-1} are also observed, which we will denote by G(k'). For these bands in Fig. 8a, b, the values of the wave vectors k'' are close to the values of $3k/4$ and $k/4$, respectively, where the wave vector k refers to the BZ border. In the region of the generalized middle component G(k') at 1481 cm^{-1} in Fig. 7a in the range 1450 – 1490 cm^{-1} a thin band structure, which characterizes the inhomogeneity of the disordered graphite-like nanostructure also observed.

In Fig. 9a, b the results of detailed numerical decomposition of the fragments of the RS of NC MoS₂(C) in the region of diamond- and graphite-like bands at a concentration of C = 1 wt.% and laser excitation at $\lambda_L = 632.8 \text{ nm}$ are shown. It is very important that with the content of C atoms increase twice, the intensity of the diamond D band at 1304 cm^{-1} in Fig. 9 in comparison with the component at 1297 cm^{-1} in Fig. 8a increased more than 4 times. On the low-

frequency wing of the D band, the weak components at 1250, 1266, and 1274 cm^{-1} of the D(k')band appear, that are shown in detail in the insert in Fig. 9a. Adjacent to the D band in Fig. 9a, the graphite-like bands G1,2(k) with frequencies of 1336 and 1355 cm^{-1} are observed. In comparison with similar bands in Fig. 8a, they are shifted towards lower frequencies, that is due to the expansion of the graphite-like phonon zone. It should be noted that they are about twice in intense and do not contain a fine structure, that indicates greater homogeneity of the structure at C = 1 wt.%.

Figure 9b shows the detailed structure of the graphite-like band in the RS of synthesized NC MoS₂(C) at C = 1 wt.% and excitation 632.8 nm. Here also the main components G and G' with frequencies 1584 and 1602, 1621 cm^{-1} are well shown, but there are also additional lines at 1567 and 1638 cm^{-1} . Figure 9b, in contrast to Figure 8b, shows a wider area in the vicinity of G band, including components 1452 and 1491 cm^{-1} of the complex middle band G(k'). In addition, Fig. 9a, b shows quite intense components of the bands G(k''). Their frequencies 1377 - 1410 cm^{-1} and 1545 cm^{-1} are close to similar components in Fig.8a, b, that confirms their reliability.

At the excitation of 488 nm for the isolated carbon band of the synthesized NC MoS₂(C) at C = 0.5 wt.% (see spectrum 1 in Fig. 6d), the maximum intensity is observed for the middle part of the spectrum, where one can select components at 1453 and 1502 cm^{-1} of G(k') band. This is the difference from the vibrational bands in Fig. 7a, b at excitation of 632.8 nm, where the maximum intensities are observed for the spaced D and G bands. We think that the high energy of photons (2.54 eV) of excitation radiation at 488 nm also gives an additional contribution to such disorder of the carbon structure at C = 0.5 wt.%. The frequency position of G band at 1579 cm^{-1} also indicates a significant disorder of the nanostructure. The large FWHM $\delta\nu \sim 130 \text{ cm}^{-1}$ of the analyzed G band indicates the size of graphite-like scales less than 1 nm.

The results of a more detailed numerical analysis of the low-frequency wing of the G(k) band, where the

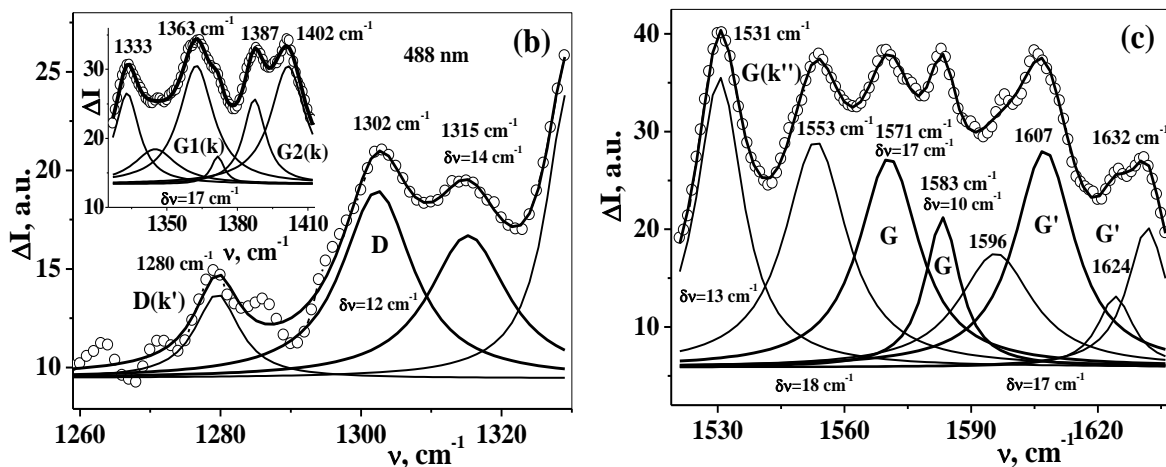


Fig. 10. The results of detailed numerical decomposition of Raman spectra fragments for NC MoS₂(C) at C = 0.5 wt.% and excitation of 488 nm in the region of diamond-shaped D bands (a) and graphite-like G bands (b) on the spectral components of the Lorentz form.

contributions of the diamond-like nanostructure should be, are shown in Fig. 10a. Here, the diamond-like D component at 1302 cm^{-1} is shifted in the low-frequency direction compared to the more intense line at 1304 cm^{-1} in Fig. 9a, due to the smaller size of the diamond-like nanostructure. And the component $D(k')$ at 1280 cm^{-1} in Fig. 10a relative to the corresponding components at 1266 and 1274 cm^{-1} in the spectrum of NC at $C = 1\text{ wt.}\%$ and excitation 632.8 nm (see insert in Fig. 9a) is offset in the high frequency direction. This clearly indicates a smaller width of the phonon band $\omega(k)$ of the diamond-like nanostructure at $C = 0.5\text{ wt.}\%$ under the action of higher-energy radiation of 488 nm .

The insert of Fig. 10a shows the structure of the complicated band $G(k)$, where the spectral components $G_{1,2}(k)$ are distinguished, respectively, with the frequencies 1363 cm^{-1} and $1387, 1402\text{ cm}^{-1}$. Note that in RS of HOPG at excitation of 488 nm the frequency of the $G_{1,2}(k)$ lines are respectively 1359 and 1376 cm^{-1} [38]. Thus, due to the smaller size and greater disorder of the studied graphite-like structure in the NC $\text{MoS}_2(C)$ at $C = 0.5\text{ wt.}\%$ the frequency of the $G_{1,2}(k)$ bands are additionally shifted towards high frequencies. Figure 10b shows the results of a detailed analysis of the structure of the RS fragment in the graphite bands G and G' for NC $\text{MoS}_2(C)$ at $C = 0.5\text{ wt.}\%$ and excitation 488 nm . Here, the observed lines G and G' have frequencies of $1571, 1583\text{ cm}^{-1}$ and 1607 cm^{-1} , that relative to similar components at 1584.7 cm^{-1} and 1610 cm^{-1} at excitation of 632.8 nm (see Fig. 8b) are shifted in the low frequency direction. This is confirmed by the shift of the components at 1531 and 1553 cm^{-1} of the $G(k'')$ band in Fig. 10b in the direction of lower frequencies relative to the corresponding components at 1546 and 1559 cm^{-1} in Fig. 8b at excitation of 632.8 nm . These facts clearly prove the narrowing of the phonon zones for the graphite-like structure in the NC $\text{MoS}_2(C)$ at $C = 0.5\text{ wt.}\%$ and $\lambda_L = 632.8\text{ nm}$.

Thus, for all decomposed bands in the Raman spectra of synthesized NC $\text{MoS}_2(C)$ with carbon additives 0.5 and $1\text{ wt.}\%$ the spectral components of diamond and graphite-like nanostructures revealed. Their changes with increasing content of C atoms and the action of laser radiation at 488 and 632.8 nm were studied.

IV. Discussion of the results

Detection of manifestations of diamond- and graphite-like structures in Raman spectra (RS) of natural and synthesized single crystals of $2H\text{-MoS}_2$, microcrystals (MC) of molybdenite, and synthesized nanocrystallites (NC) of $\text{MoS}_2(C)$ with small carbon additives indicates the ability of layered structures of transition metal dichalcogenides (TMD) to include carbon in its structure. Moreover, the special structure-forming ability of $2H\text{-MoS}_2$ structures from nano to macro sizes to form diamond-like and graphite-like nanostructures with previously little-studied properties has been established. It is known that by thermal annealing in air of nanodiamonds (ND) at a temperature about $500\text{ }^\circ\text{C}$ it is possible to clean them from the non-

diamond shell and reduce their size [77]. It turned out that the purified and reduced crystalline ND remained stable up to 1.1 nm , and at sizes less than 1 nm they amorphized. Our spectral studies allowed us to establish the existence of diamond-like structures with low frequencies of $1284, 1295 - 1312\text{ cm}^{-1}$ and sizes less than 1 nm . Probably, their presence in the synthesized single crystals and agglomerates of NC $\text{MoS}_2(C)$ enhances their stability, as well as the stability of graphite-like structures with vibrational G lines had FWHM $\delta\nu \sim 10\text{ cm}^{-1}$, that is comparable or even smaller than in single crystals of HOPG. The evolution of diamond- and graphite-like nanostructures to quasi-molecular sizes opens new perspectives for research and applications from nonlinear quantum physics to biomedicine [78, 79].

We found a change in the electronic states of NC $\text{MoS}_2(C)$ under the action of resonant with exciton states radiation of 632.8 nm , including amplification of the broadband electron background, anomalous amplification of overtones and sum tones and formation of molybdenum trioxide $\alpha\text{-MoO}_3$ with characteristic strong lines at 818 and 991 cm^{-1} (see Fig. 6b), as well as a significant enrichment of the spectrum of low-frequency vibrations (Fig. 6a) opens a new direction for changing and controlling the electronic properties of nanoparticles. The manifestations in the Raman spectra the acoustic modes of NC $\text{MoS}_2(C)$, the appearance in this region the low-frequency vibrations of $\alpha\text{-MoO}_3$, as well as the presence of higher-frequency vibrational resonances of carbon nanostructures and adsorbed water contributes to efficient pumping of thermal energy associated with strong VEI [14 - 17]. In particular, it was shown in [80] that diamond-like carbon and thermally annealed diamond thin films exhibit SERS activity without any metal nanostructures on their surfaces, which is undoubtedly associated with changes in electronic states.

The observation of three characteristic spectral features of diamond-like states, namely spectral components D , $D(k)$ and $D(k')$ with frequencies $\nu = 1285 - 1315\text{ cm}^{-1}$; $1224 - 1280\text{ cm}^{-1}$ and $1168 - 1180\text{ cm}^{-1}$, respectively, are strong evidence of the formation of nanostructures with sp^3 -hybridization and manifestations of their collective nature, including the formation of diamond-like phonon zones. It should be noted that onion-like structures are also formed for MoS_2 NCs [21, 81, 82], that due to internal self-compression can play the role of nanopresses for HA synthesis [7]. To convince the conclusion about the emergence of diamond- and graphite-like structures in the synthesized NC $\text{MoS}_2(C)$, we compared our selected spectral components with the position of the bands $G(k)$ in the RS of single-walled (SWNT) and multiwall (MWNT) carbon nanotubes, from the edges of HOPG and implanted with C^+ ions graphite (CHOPG). We used experimental data obtained in [38, 52, 83]. Figure 11 shows the change in the frequencies of the $G(k)$ bands in the RS in such sequence of carbon materials: SWNT, HOPG, MWNT and CHOPG at excitation of 632.8 nm (curve 1) and 488 nm (curve 2). The minimum values of the frequencies of $G(k)$ bands in the case of excitation at 632.8 nm equal to 1323 and 1324 cm^{-1} are achieved in the Raman spectrum of SWNT and from the HOPG edge, ie they can overlap with the D lines of ND. In more

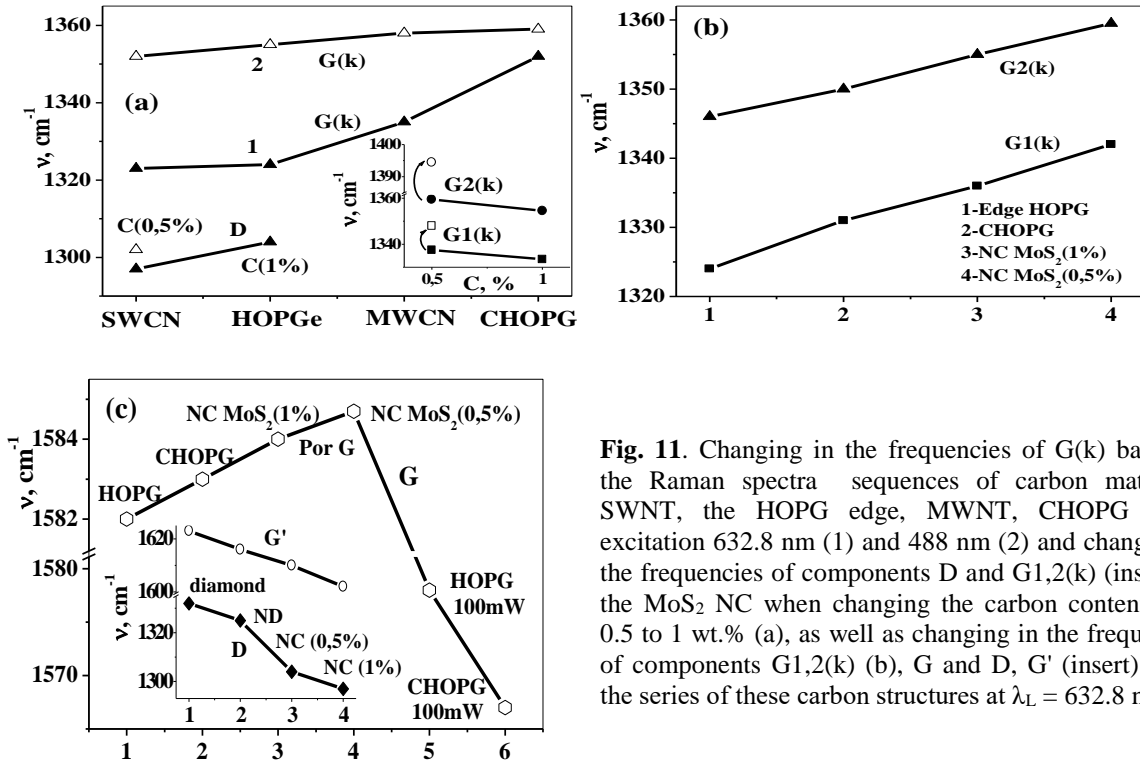


Fig. 11. Changing in the frequencies of G(k) bands in the Raman spectra sequences of carbon materials: SWNT, the HOPG edge, MWNT, CHOPG under excitation 632.8 nm (1) and 488 nm (2) and changing in the frequencies of components D and G1,2(k) (insert) in the MoS₂ NC when changing the carbon content from 0.5 to 1 wt.% (a), as well as changing in the frequencies of components G1,2(k) (b), G and D, G' (insert) (c) in the series of these carbon structures at $\lambda_L = 632.8$ nm.

disordered samples of MWNT and CHOPG, the frequencies of G(k) bands increase to 1335 and 1352 cm^{-1} , respectively, and are well separated from the D lines by ND. In the case of using excitation of 488 nm for all considered carbon materials G(k) bands are located above 1350 cm^{-1} .

Figure 11,a shows the change in the frequency of D lines of diamond-like structures in NC MoS₂(C) with increasing carbon concentration from 0.5 to 1 wt.% and the excitations of 488 and 632.8 nm. It is seen that the decrease of the frequencies of D lines to the values of 1297 and 1304 cm^{-1} allows us to confidently separate them from the components of the graphite-like nanostructures analyzed by us. The insert in Fig. 11a shows the change in the frequencies of the components G1(k) and G2(k) corresponding to the optical modes of graphite TO (K) and LO (M) at points K and M at the edges of BZ, with increasing carbon content in NC MoS₂(C) from 0.5 to 1 wt.% and $\lambda_L = 632.8$ nm. As the concentration of C atoms increases, the frequencies of G1,2(k) decrease at $\sim 4 - 5$ cm^{-1} , and the frequencies of D lines, on the contrary, increase at ~ 7 cm^{-1} , that confirms their correspondence to different structures. This change in the frequencies of the components D and G1,2(k) is due to the expansion of the corresponding phonon zones $\omega(k)$, for which the D line is top of zone and the bands G1,2(k) are in the bottom.

Significant ordering of graphite- and diamond-like structures at a carbon content of 1 wt.% follows from the weakening of G(k) band in Fig. 7b and the strengthening of the D component more than 4 times, as well as reducing its FWHM $\delta\nu$ more than 2 times. In addition, the vibrational frequencies of diamond-like structures are practically independent of the photon energy of the

excitation radiation. Thus, for NC MoS₂(C) with a carbon content 0.5 wt.%, the frequency of D line is 1297 cm^{-1} at excitation 632.8 nm, and at 488 nm – 1302 cm^{-1} (see the lower left edge of Fig. 11a). At the same time, for all graphite-like materials, the frequencies of the G(k) bands increase significantly when using laser radiation with higher photon energy, that is illustrated in Fig. 11a. In particular, the frequencies of the components G1,2(k) at excitation 488 nm increase by 10 and 35 cm^{-1} , as shown by the arrows in the insert of Fig. 11a. The increase in the frequencies of G1,2(k) bands from 1359 and 1376 cm^{-1} at $\lambda_L = 488$ nm [38] to the values of 1363, 1387 and 1402 cm^{-1} in NC MoS₂ (C = 0.5 wt.%) (See the insert in Fig. 10a) indicates a record increase in the lower edges of graphite-like phonon zones. In fact, the independence of the frequencies of the D lines from the values of λ_L , the observation of D(k) and D(k') bands, as well as the opposite dependences of the frequencies of components D and G1,2(k) on the concentration of carbon additives in NC MoS₂(C) are convincing evidence of the existents of diamond-like states.

The strict separation of the D lines of nanodiamond (ND) in the center of BZ and its graphite-like shell at the edge of the BZ G(k), which overlap, was previously performed using IR spectroscopy [43 - 45]. The use of IR spectra, in addition to achieving a good signal-to-noise ratio, also has the advantage that the position of the G(k) bands in the IR spectra does not change, as in the Raman spectra. It is significant that the IR absorption of the diamond core and its graphite shell increases abnormally with increasing annealing temperature of detonation ND to $\sim 1000^\circ$ [43 - 45], that is especially evident for D(k) band. The observed frequencies of G1,2(k) lines 1353 and 1372 cm^{-1} correspond to the oscillating modes

TO(K) and LO(M) at points K and M at the edges of BZ. These frequencies are very close to the results of [37, 38] at excitation of 515.5 nm for CHOPG (1350, 1368 cm^{-1}) and the edge of HOPG (1352 and 1369 cm^{-1}), where there is no identification of the observed bands. But it is important that these frequencies are higher than the frequencies of these modes for HOPG samples under normal conditions, which are determined by the inelastic scattering of X-rays TO(K) = 1265 cm^{-1} and LO(M) = 1323 cm^{-1} [49]. Thus, the effect of 514.5 nm laser radiation leads to the same high-frequency displacements of the vibrational bands G1,2(k) as the thermal annealing of ND at a temperature of 1000 °C.

The formation of diamond-like and graphite-like nanostructures with record low values of D components and high frequencies of G1,2(k) bands in NC MoS₂(C) opens the prospect of analyzing changes in the frequencies of different vibrational states of diamond and graphite structures at their maximum disorder, that is illustrated in Fig. 11b, c. Figure 11b shows a significant increase in the frequencies of the vibrational components G1(k) and G2(k), corresponding to the modes TO(K) and LO(M), with sequential disordering of the structure from the edge of the HOPG and CHOPG [37, 38] to the NC MoS₂(C) with a carbon content of 1 and 0.5 wt.%. In this case the frequencies of G1,2(k) increase by 15 - 18 cm^{-1} , that is much larger than their change when changing the excitation 514.5 nm to 488 nm (8 - 9 cm^{-1}). This example shows the feasibility of studying the low concentrations of C atoms ~ 0.5 wt.% and the choice of such a sequence of carbon structures, for which the frequencies of the bands G1,2 (k) are approximately equidistant.

Figure 11c shows the frequency changes of the main graphite line G (1582 cm^{-1} in HOPG), as well of the fundamental diamond D line 1332 cm^{-1} and the high-frequency satellite G' of line G (1623 cm^{-1} from the edge of HOPG) [37] in similar series of materials with the disorganization of the structure. In particular, the frequency of the fundamental line G during the disordering of graphite initially increases and reaches a maximum value of 1584 - 1585 cm^{-1} in NC MoS₂(C) under study and nanoporous graphite [42]. The strong decrease in the frequencies of G lines under the action of 514.5 nm laser radiation with increased power to 100 mW is very interesting [38, 52]. The change in the excitation frequency is insignificant here when the frequency G of the line is reduced by 38 cm^{-1} , since it is assumed that these lines are not shifted when changing λ_L . According to the ratio of the intensities of the Stokes and anti-Stokes components of the G lines, the authors [38, 52] determined the temperatures of 647 and 815 K in HOPG and CHOPG, that is not entirely correct, because according to our data in resonant Raman scattering in graphite and graphene, as in NC samples MoS₂(C) [13, 84] the processes of stimulated scattering begin to develop even at lower laser radiation powers. This is confirmed by a significant difference in the frequencies of the Stokes and anti-Stokes components G1,2(k) ~ 7 cm^{-1} at excitation of both 632.8 nm and 488 nm [38]. In addition, the intense laser radiation leads to significant changes in the structure and properties of matter [12, 55, 85].

The insert in Fig. 11c shows approximately the same

anomalous decrease in the frequency of the diamond-like D line ~ 35 cm^{-1} in the diamond-like nanostructures observed by us in the MoS₂(C) NC. For component G' there is also a decrease in frequency by more than 20 cm^{-1} in NC MoS₂(C) with low carbon additives. In contrast to the increase in frequencies G1,2(k) in Fig. 11b, that are associated with the bottom of the graphite-like phonon band $\omega(k)$, the frequencies of the components D, G and G' associated with the upper edges of the corresponding phonon bands decrease; that should be when the width of the phonon zones reduces.

Let's analyze the possible physical mechanisms of formation of diamond-like nanostructures in MoS₂(C). It is known that in thin layers and nanoparticles of many substances can be stable structures that are metastable for massive samples, including the structures characteristic for high-pressure phases [86]. The unique properties of NC MoS₂(C), including the excitation of higher vibrational states, due to the nonlinear resonant interaction of thermally excited vibrational modes and amplification of VEI [14 - 17], significantly activate the substance, contributing to favorable conditions for high pressure phase synthesis. In particular, this is manifested in the transformation of nanostructures MoS₂ → MoO₃ under the influence of low-power 632.8 nm laser radiation (see Fig. 6b). An anomalous increase in the intensity of the overtones of the valence vibrations of water ν_{OH} and the strongest dipole mode of quartz ν_3 (F2) was observed earlier in our papers [79, 87, 88]. The presence of carbon, as well as the additional formation of various defects in the structure of the NC MoS₂(C) leads to an increase in wave nonlinearity. As a result of the spatiotemporal accumulation of nonlinear wave effects, even weak wave nonlinearity leads to significant phenomena (for example, complete conversion of laser radiation into harmonics or Stokes radiation with stimulated Raman scattering).

In the monograph [86] it is reported the obtaining of stable clusters of carbon and metal atoms M₈C₁₂ (M = Ti, V, Zr, Nb, Hf, Cr, Mo) with symmetry close to T_d. In the IR spectra of such clusters, strong absorption bands were observed in the region of D bands of diamond and G(k) of graphite. In particular, an infrared band at ~ 1300 cm^{-1} was observed for Zr₈C₁₂ clusters. It is possible that in the MoS₂(C) NC, molybdenum atoms can form chemical bonds not only with sulfur atoms, but also with impurity carbon atoms, giving rise to the formation of sp³ hybridization and synthesis of diamond-like inclusions. In another paper [42], devoted to the production and study of nanoporous graphite, it is believed that sp³ bonds can be formed between graphite planes at the edges of nanoparticles.

It should be noted the work on the controlled production of diamond- or graphite-like nanostructures using SiC superstructures [89]. The crystallization processes in initially amorphous multilayer SiC superlattices with a layer thickness of 1.6 and 3.2 nm, alternating with spraying with carbon layers with a thickness of 0.8 and 1.34 nm, were studied. The thicknesses of the carbon layers were selected as multiples of the interplanar distances in diamond in the direction (111) (a = 0.205 nm) and graphite in the direction (002) (a = 0.335 nm). Depending on the

geometric parameters of the superlattice, diamond-like or graphite-like structures were formed during high-speed annealing, controlled by Raman and photoluminescence spectra.

MoS₂ monolayers with a thickness of 0.32 - 0.35 nm and with distances between monolayers of 0.67 nm [23] also represent a short-period superlattice, in which in the presence of carbon the conditions for the formation of diamond- and graphite-like nanostructures can be created. Significant low-frequency displacements of the observed D components relative not only to the diamond line 1332 cm⁻¹, but also to the lines of ND 1322 - 1326 cm⁻¹ are associated with the very small size of the formed diamond-like nanostructures. This is confirmed by the similarity of the structure of the Raman spectra in Fig. 6a, b and in [85], where the diamond-like phase synthesis under the influence of femtosecond laser pulses (25 fs) on polycrystalline graphite realized, that was confirmed by high resolution electron microscopy and electron diffraction.

At the end of the discussion of the problem of synthesis of diamond-like nanostructures, it should be noted that this discussion is not about obtaining an equilibrium bulk phase of matter, but about metastable nanostructured formations, for which the possible phase transitions are realized at several discrete stages distributed over a wide temperature range [90, 91]. The substances in intermediate states in these discrete transformations of the structure can obtain special unique properties that are not realized in equilibrium conditions, such as increased strength characteristics or abnormally high intensities in the vibrational spectra [45, 90, 91]. The versatility of the considered phenomena in NC MoS₂(C) is associated with the effects of nonlinear quantum self-compression of matter [92], as well as the effect of laser radiation on the structure and properties of matter when recording Raman spectra [38, 52, 55, 93], which was partially analyzed above. In [92], the collapse of the wave functions of an anharmonic oscillator during excitation of higher vibrational states (vibrational quantum level $v \geq 4.5$) was established for the first time, that explains the universal mechanism of internal self-compression.

All this facts indicates the need for further studies of the conditions for the synthesis of diamond-like states of carbon in various nanostructures and superlattices without the explicit use of high pressures and temperatures, which is both fundamental and practical importance.

Conclusions

1. The existence of diamond-like and graphite-like nanostructures in crystals of natural molybdenite and synthesized 2H-MoS₂ single crystal with uncontrolled small carbon impurities was shown for the first time. These carbon nanostructures in synthesized nanocrystallites of MoS₂(C) with 0.5 and 1 wt.% C-content were studied in detail. In Raman spectra (RS) at laser excitation of 488 nm for diamond-like nanostructures the record low frequencies of D lines 1284, 1295 - 1312 cm⁻¹ (weakly dependent on the

frequency of excitation radiation) were observed, and for graphite-like nanostructures the high frequencies of G(k) bands 1387 and 1402 cm⁻¹ were recorded, corresponding to the vibrational states at the borders of the Brillouin zone and dimensions less than 1 nm. The record values of the frequencies of D and G(k) components of carbon nanostructures are associated with the narrowing of the corresponding phonon zones. Both the direct chemical bond of Mo and C atoms and the special cooperative properties of short-period superlattices can be important for the formation of these nanostructures [89].

2. A new method for separating the spectral components of overlapping diamond-like and graphite-like structures $D \approx G(k)$ is proposed and used, taking into account the shifts of these components toward lower and higher frequencies while decreasing the size and increasing the disorder of the substance. It is shown that these frequency changes are caused by a decrease in the widths of the corresponding phonon zones.

3. The gain of D bands of diamond-like structure ~ 4 times and significant ordering of graphite-like structure with increasing of carbon content in NC MoS₂(C) from 0.5 to 1 wt.%. Observation in the Raman spectra of sets of discrete spectral components G(k), G(k') and G(k'') of graphite-like structures and D(k) and D(k') components of diamond-like structures proves that their disorientation is mainly by a sequence of processes doubling the size of elementary quasi-cells.

4. For the first time, a significant change in the electronic states of the MoS₂(C) NC under the action of resonant with excitonic states laser radiation of 632.8 nm was established. This is manifested in the strengthening of the broadband electronic background, oxidation of the structure of NC MoS₂(C) with the formation of molybdenum trioxide α -MoO₃, that leads to the activation of the formation and ordering of diamond-like and graphite-like nanostructures with the participation of nanocomposite MoS₂ + MoO₃. The change of electronic states is largely associated with the excitation of higher vibrational states and the effects of strong vibrational-electronic interaction [14-17], that shows the way to control the electronic properties of nanoparticles.

5. It is established that the increased values of the frequencies of the G(k) spectral components in the Raman spectra of graphite-like structures and even HOPG, differ significantly from the data of inelastic X-ray scattering. This is due to changes in the structure and properties of the substance under the action of intense laser radiation. In particular, the laser radiation of 514.5 nm leads to the same high-frequency displacements of the TO (K) and LO (M) vibrational bands of the graphite structure, as well as the thermal annealing of nanodiamonds at a temperature of 1000 °C.

Acknowledgments

The authors express their gratitude to Dr. Sc., Prof. Fedorov V.E. (A.V. Nikolaev Institute of Inorganic Chemistry, Novosibirsk) for providing data on the Raman spectrum of the 2H-MoS₂ single crystal synthesized by him; Ph.D. Melnik N.N. (P.N. Lebedev Institute of Physics, Moscow) for information on the spectral properties of porous graphite and special

structure-forming properties of short-period superlattices; Ph.D. Axelrud L.G. (Ivan Franko National University of Lviv, Lviv) for performing X-ray examinations; Ph.D. Koenig-Ettel N.B. (I.M. Frantsevich Institute for Problems of Materials Science, Kyiv) for sample preparation.

Kornienko M.E. - PhD, senior researcher, senior researcher at the Research Institute of Electro-Optical Processes of the Faculty of Physics;
Naumenko A.P. - PhD, senior researcher, head of the Research Institute of Electro-Optical Processes of the Faculty of Physics;
Kulikov L.M. - Doctor of Technical Sciences, Senior Researcher, Head of the Department of Fine Inorganic Synthesis, Thermodynamics and Kinetics of Heterophase Processes.

- [1] M. Samadi, N. Sarikhani, M. Zirak, H. Zhang, H.-L.Zhang, A. Z. Moshfeg, *Nanoscale Horiz.* 3(3), 90 (2018) (<https://doi.org/10.1039/c7nh00137a>).
- [2] J. Ping, Z. Fan, M. Sindoro, Y. Ying, and H. Zhang, *Adv. Funct. Mater.* 27(19), 1605817 (2017) (<https://doi.org/10.1002/adfm.201605817>).
- [3] Q. Lv, Ruitao Lv, *Carbon*, 145, 240 (2019) (<https://doi.org/10.1016/j.carbon.2019.01.008>).
- [4] X. Zong, H. Yan, G. Wu, G. Ma, F. Wen, L. Wang, and C. Li, *J. Am. Chem. Soc.* 130(23), 7176 (2008) (<https://doi.org/10.1021/ja8007825>).
- [5] T. Daeneke, N. Dahr, P. Atkin, R.M. Clark C.J. Harrison, et.al., *ACS Nano* 11(7), 6782 (2017). (<http://pubs.acs.org/doi/abs/10.1021/acsnano.7b01632>).
- [6] N.E. Kornienko, *Ukr. J. Phys.* 47(4), 361 (2002).
- [7] F. Banhart, P.M. Ajayan, *Nature* 382, 433 (1996) (<https://doi.org/10.1038/382433a0>).
- [8] Anke Krueger, *Carbon Materials and Nanotechnology*, (WILEY-VCH Verlag GmbH, Weinheim, 2010) (<https://doi.org/10.1002/9783527629602.ch7>).
- [9] F. Banhart, *Phys. Sol. State* 44(3), 399 (2002) (<https://doi.org/10.1134/1.1462655>).
- [10] L.T. Daulton, M.A. Kirk MA, R.S. Lewis, L.E. Rehn, *Nucl. Inst.Meth. Phys. Res. B* 175-177, 12 (2001) (DOI: [10.1016/S0168-583X\(00\)00603-0](https://doi.org/10.1016/S0168-583X(00)00603-0)).
- [11] P. Wesolowski, Y. Lyutovich, F. Banhart, H. D. Carstanjen and H. Kronmuller, *Appl. Phys. Lett.*, 71(15), 1948 (1997) (<https://doi.org/10.1063/1.119990>).
- [12] R. Nu'ske, A. Jurgilaitis, H. Enquist, M. Harb, Y. Fang, U. Hakanson, and J. Larsson, *Appl. Phys. Lett.* 100(4), 043102 (2012).
- [13] N.E. Kornienko, A.P. Naumenko, V.O. Gubanov, V.E. Fedorov., S.B. Artemkina, *International research and particle conference Nanotechnology and Nanomaterials (NANO-2019) (Lviv, Ukraine, 2019)*.
- [14] N.E. Kornienko, *Visnyk Kyivskogo Universytetu [Kyiv University Bulletin]* 3, 489 (2006) (in Ukrainian).
- [15] N.E. Kornienko, N.P. Kulish, S.A. Alekseev, O.P. Dmitrenko, and E.L. Pavlenko, *Optics and Spectroscopy*, 109(5), 742 (2010) (<https://doi.org/10.1134/S0030400X10110147>).
- [16] M. Kornienko, A. Naumenko, *Ukr. J.Phys.* 59(3), 339 (2014) (<https://doi.org/10.15407/ujpe58.02.0151>).
- [17] N.E. Kornienko and A.P. Naumenko, *Chemical Functionalization of Carbon Nanomaterials: Chemistry and Application* (Eds. V.K.Thakur and M.K.Thakur) (Boca Raton–London–New York: CRC Press: 2015), chapter 5, 103 (2015).
- [18] V.V. Sobolev, V.V. Nemoshkalenko. *Methods of computational physics in the theory of solids* (Kiev, Naukova dumka, 1990) (In Russian).
- [19] X. Zhang, X.-F. Qiao, W. Shi, J.-B. Wu, D.-S. Jiang, and P.-H. Tan, *Chem. Soc. Rev.* arXiv:1502.00701v1 [cond-mat.mtrl-sci] 3 Feb 2015.
- [20] X. Zhang, W.P. Han, J.B. Wu, S. Milana, Y. Lu, Q.Q. Li, A.C. Ferrari, and P.H. Tan, *Phys. Rev. B*, 87(11), 115413 (2013) (<https://doi.org/10.1103/PhysRevB.87.115413>).
- [21] G.L. Frey, R. Tenne, M.J. Matthews, M.S. Dresselhaus, G. Dresselhaus, *Phys. Rev. B* 60(4), 2883 (1999) (<https://doi.org/10.1103/PhysRevB.60.2883>).
- [22] J.M. Chen and C.S. Wang, *Solid State Communications*, 14(9), 857 (1974) ([https://doi.org/10.1016/0038-1098\(74\)90150-1](https://doi.org/10.1016/0038-1098(74)90150-1)).
- [23] B.C. Windom, W.G. Sawyer, D.W. Hahn, *Tribol Lett.* 42(3), 301 (2011) (<https://doi.org/10.1007/s11249-011-9774-x>).
- [24] C. Ataca, M. Topsakal, E. Akturk, and S. Ciraci, *J. Phys. Chem. C* 115(33), 16354 (2011) (<https://doi.org/10.1021/jp205116x>).
- [25] *Light Scattering in Solids II. Basic Concepts and Instrumentation*, Edited by M. Cardona and G.Guntherodt (Springer-Verlag, Berlin-Heidelberg-New York, 1982).
- [26] L. Akselrud, Y. Grin, *J. Appl. Crystallogr.* 47(2), 803 (2014) (<https://doi.org/10.1107/S1600576714001058>).
- [27] *Preparation and crystal growth of materials with layered structures*, R.M.A. Lieth (ed.), (Dordrecht-Boston, 1977), chapter 4, R.M.A. Lieth, J.C.J.M. Terhell. *Transition Metal Dichalcogenides*, 141-223 (https://doi.org/10.1007/978-94-017-2750-1_4).
- [28] I.G. Vasilyeva, I.P. Asanov, L.M. Kulikov. *J. Phys. Chem. C*, 119(40), 23259 (2015) (<https://doi.org/10.1021/acs.jpcc.5b07485>).

- [29] A. Naumenko, L. Kulikov, N. Konig, *Ukr. J. Phys.* 61(6), 556 (2016) (<https://doi.org/10.15407/ujpe61.06.0561>).
- [30] S.S. Bukalov, L.A. Leites, R.R. Aysin, *Advanced Materials Letters* 10(8), 550(2019) (<https://doi.org/10.5185/amlett.2019.2268>).
- [31] A.P. Naumenko, N.E. Kornienko, V.M. Yashchuk, V.N. Bliznyuk, S. Singamaneni, *Ukr. J. Phys.* 57(2), 197 (2012).
- [32] A.P. Naumenko, N.E. Korniyenko, V.N. Yaschuk, S. Singamaneni, and V.N. Bliznyuk, *Raman Spectroscopy for Nanomaterials Characterization*, C. Kumar (ed.) (Springer-Verlag, Berlin Heidelberg, 2012).
- [33] O.Yu. Posudievsky, O.A. Khazieieva, V.V. Cherepanov, G.I. Dovbeshko, A.G. Shkavro, V.G. Koshechko, and V.D. Pokhodenko, *J. Mater. Chem. C* 1(39), 6411 (2013).
- [34] A.C. Ferrari and J. Robertson, *Phys. Rev. B*, 64(7), 075414 (2001) (<https://doi.org/10.1103/PhysRevB.64.075414>).
- [35] A.C. Ferrari and J. Robertson, *Phil. Trans. R. Soc. Lond. A* 362(1824), 2477 (2004) (<https://doi.org/10.1098/rsta.2004.1452>).
- [36] O.O. Mykhaylyk, Y.M. Solonin, D.N. Batchelder, R. Brydson, *J. Appl. Phys.* 97(7), 074302 (2005). (<https://doi.org/10.1063/1.1868054>).
- [37] P.H. Tan, S. Dimovski and Y. Gogotsi, *Phil. Trans. R. Soc. Lond. A*, 362, 2289 (2004) (<https://www.jstor.org/stable/4488953>).
- [38] P.H. Tan, Y.M. Deng, and Q. Zhao, *Phys. Rev. B*, 58(9), 5435 (1998).
- [39] C. Thomsen and S. Reich, *Phys. Rev. Lett.* 85(24), 5214 (2000).
- [40] C. Thomsen and S. Reich, *Phil. Trans. R. Soc. Lond. A* 362(1824), 2271 (2004).
- [41] M.A. Pimenta, G. Dresselhaus, M.S. Dresselhaus, L.G. Canc ado, A. Jorio and R. Saito, *Phys. Chem. Chem. Phys.* 9(11), 1276 (2007) (<https://doi.org/10.1039/B613962K>).
- [42] V.A. Karavanskii, N.N. Mel'nik T.N. Zavaritskaya, *JETP Lett.* 74(3), 186 (2001) (<https://doi.org/10.1134/1.1410227>).
- [43] N.E. Kornienko, A.D. Rud, A.N. Kirichenko, *Izvestiya vuzov, Chimiya i chimicheskaya technologiya* 58(5), 25 (2015).
- [44] N.E. Kornienko, A.D. Rud, A.N. Kirichenko In: "Carbon: Fundamental Problems of Science, Material Research, Technology" (Proceedings of 9-th International Conference, Moscow, Troitsk, 2014).
- [45] N.E. Kornienko, A.N. Kirichenko, In: *Proceedings of XXV Congress on Spectroscopy (Moscow-Troitsk, 2016)*. P. 291.
- [46] A.L. Vereshchagin, *The properties of detonated diamonds* (Barnaul, 2005).
- [47] H. Motahari and R. Malekfar, *International Journal of Optics and Photonics (IJOP)* 13(1), 3 (2019).
- [48] S. Osswald, V.N. Mochalin, M. Havel, G. Yushin, and Y. Gogotsi, *Phys. Rev.* 80(7), 075419 (2009) (<https://doi.org/10.1103/PhysRevB.80.075419>).
- [49] J. Maultzsch, S. Reich, C. Thomsen, H. Requardt, and P. Ordejo'n, *Phys. Rev. Lett.* 92(7), 075501 (2004) (<https://doi.org/10.1103/PhysRevLett.92.075501>).
- [50] L. Gustavo de O. L. Cancado, *Raman spectroscopy of nanographites* (Setembro de, 2006).
- [51] *Light Scattering in Solids III. Recent Results*, Edited by M. Cardona and G. Guntherodt (Springer-Verlag, Berlin-Heidelberg-New York, 1982).
- [52] P.H. Tan, Y.M. Deng, and Q. Zhao, and W.C. Cheng, *Appl. Phys. Lett.* 74(13), 1818 (1999).
- [53] P. Giura, N. Bonini, G. Creff, J.B. Brubach, P. Roy, and M. Lazzeri, *Phys. Rev. B* 86(12), 121404(R), (2012) (<https://doi.org/10.1103/PhysRevB.86.121404>).
- [54] Y.A. Kim, H. Muramatsu, T. Hayashi, M. Endo, M. Terrones, M.S. Dresselhaus, *Chem. Phys. Lett.* 398: 87 (2004) (<https://doi.org/10.1016/j.cplett.2004.09.024>).
- [55] K. Witke, D. Klaffke, A. Skopp and J. P. Schreckenbach, *J. of Raman Spectroscopy* 29, P. 411 (1998).
- [56] Y. Kawashima, G. Katagiri, *Phys. Rev. B*, 52(14), 10053 (1995).
- [57] Y. Kawashima, G. Katagiri, *Phys. Rev. B* 59(1), 62 (1999).
- [58] L. Bokobza, J. Zhang, *eXPRESS Polymer Letters* 6(7), 60 (2012) (<https://doi.org/10.3144/expresspolymlett.2012.63>).
- [59] N.E. Kornienko, A.P. Naumenko, L.M. Kulikov, *Nanosistemi, Nanomateriali, Nanotehnologii*, 18(1), 15 (2020).
- [60] M. Ikram, R. Tabassum, U. Qumar, S. Ali, A. Ul-Hamid, A. Haider, A. Raza, M. Imranf and S. Ali, *RSC Adv.*, 10(35), 20559 (2020) (<https://doi.org/10.1039/d0ra02458a>).
- [61] Hsiang-Lin Liu, Huaihong Guo, Teng Yang, Zhidong Zhang, Yasuaki Kumamoto, Chih-Chiang Shen, Yu-Te Hsu, Lain-Jong Li, Riichiro Saito and Satoshi Kawatadg, *Phys. Chem. Chem. Phys.* 17, 14561 (2015) (<https://doi.org/10.1039/c5cp01347j>).
- [62] D.N. Khaemba, A. Neville and A. Morina, *Tribology Letters*, 59(3), 1 (2015) (<https://doi.org/10.1007/s11249-015-0566-6>).
- [63] A. Jagminas, G. Niaura, R. Žalneravičius, R. Trusovas, G. Račiukaitis, V. Jasulaitiene, *Sci Rep* 6(1), 37514 (2016) (<https://doi.org/10.1038/srep37514>).
- [64] T. Wang, J. Li, G. Zhao, *Powder Technol.* 253(2), 347 (2014).

- [65] M.A. Camacho-López, L. Escobar-Alarcón, M. Picquart, R. Arroyo, G. Córdoba, E. Haro-Poniatowski, *Optical Mater.* 33(3), 480 (2011) (<https://doi.org/10.1016/j.optmat.2010.10.028>).
- [66] Latha Kumari, Yuan-Ron Ma, Chai-Chang Tsai, Yi-Way Lin, Sheng Yun Wu1, Kai-Wen Cheng and Yung Liou, *Nanotechnology* 18(11), 115717 (2007) (<https://doi.org/10.1088/0957-4484/18/11/115717>).
- [67] Hongfei Liu, K. K. Ansah Antwi, Chengguo Li, Jifeng Ying, Soojin Chua, and Dongzhi Chi, *Nanotechnology* 25(40), 405702 (2014) (<https://doi.org/10.1088/0957-4484/25/40/405702>).
- [68] Y. Lin, W. Zhang, J. Huang, K. Liu, Y. Lee, C. Liang, C. Chu, L. Li, *Nanoscale* 4(2), 6637 (2012) (<https://doi.org/10.1039/c2nr31833d>).
- [69] Bing Han, Yun Hang Hu, *Energy Science & Engineering*, 4(5), 285 (2016).
- [70] W. Su, P. Wang, Z. Cai, J. Yang, X. Wang, *Results in Physics*, 12(3), 250 (2019) (<https://doi.org/10.1016/j.rinp.2018.11.066>).
- [71] M. Ikram, M.I. Khan, A. Raza, M. Imran, A. Ul-Hamid, S. Ali, *Physica E: Low-dimensional Systems and Nanostructures*, 124(8), 114246 (2020) (<https://doi.org/10.1016/j.physe.2020.114246>).
- [72] A. Chithambararaj, N.S. Sanjini, S. Velmathib and A. Chandra Bose, *Phys. Chem. Chem. Phys.*, 15(35), 14761 (2013) (<https://doi.org/10.1039/C3CP51796A>).
- [73] Chao Hu, Minjie Xu, Jun Zhang, Yunong Zhou, Bonian Hu, Gang Yu, *Chemical Kinetics* 5(1), 3 (2019)
- [74] Z. Chen, D. Cummins, B.N. Reinecke, E. Clark, M.K. Sunkara, T.F. Jaramillo, *Nano Lett.* 11(10), 4168 (2011) (<https://doi.org/10.1021/nl2020476>).
- [75] N. Zamora-Romero, M.A. Camacho-Lopez, A.R. Vilchis-Nestor, V.H. Castrejon-Sanchez, G. Aguilar, S. Camacho-Lopez, M. Camacho-Lopez, *Materials Chemistry and Physics*, 240 122163 (2020).
- [76] N. Kumar, B.P.A. George, H. Abrahamse, V. Parashar, J.C. Ngila, *Appl. Surf. Sci.*, 396(2), 8 (2017) (<https://doi.org/10.1016/j.apsusc.2016.11.027>).
- [77] S. Stehlik, M. Varga, M. Ledinsky, D. Miliaieva, *Sci Rep* 6(12), 38419 (2016). (<https://doi.org/10.1038/srep38419>).
- [78] N.E. Kornienko, *Physics of the Alive* 16(1), 5 (2008).
- [79] N.E. Kornienko, *Physics of the Alive* 17(2), 5 (2009).
- [80] M.K. Kuntumalla, V.V.S. Siva Srikanth, S. Ravulapalli, U. Gangadharini, H. Ojha, N.R. Desai and C. Bansal, *Phys. Chem. Chem. Phys.* 17(33), 21331 (2015) (<https://doi.org/10.1039/C4CP05236F>).
- [81] M. Levy, A. Albu-Yaron, R. Tenne, D. Feuermann, E.A. Katz, D. Babai, and J.M. Gordon, *Israel J. Chem.* 50(4), 417 (2010) (<https://doi.org/10.1002/ijch.201000056>).
- [82] M. Chhowalla, G.A.J. Amaratunga, *Nature* 407(6801), 164 (2000) (<https://doi.org/10.1038/35025020>).
- [83] P.H. Tan, L. An, L.Q. Liu, Z.X. Guo, R. Czerw, D.L. Carroll, P.M. Ajayan, N. Zhang, and H.L. Guo, *Phys. Rev. B.* 66(24), 245410 (2002) (<https://doi.org/10.1103/PhysRevB.66.245410>).
- [84] V.V. Strelchuk, A.S. Nikolenko, V.O. Gubanov, M.M. Bilyi, and L.A. Bulavin, *Journal of Nanoscience and Nanotechnology* 12(11), 8671 (2012) (<https://doi.org/10.1166/jnn.2012.6815>).
- [85] F.C.B. Maia, R.E. Samad, J. Bettini, R.O. Freitas, N.D.V. Junior, N.M. Souza-Neto, *Scientific Reports* 5(1), 11812 (2015) (<https://doi.org/10.1038/srep11812>).
- [86] J.A. Alonso, *Structure and Properties of Atomic Nanoclusters* (Universidad de Valladolid, Spain, 2nd Edition, by Imperial College Press, 2012).
- [87] N.E. Korniyenko, N.P. Smolyar, *Abstracts of XVI-th Int. School-Seminar "Spectroscopy of Molec. and Crystals* (Sevastopol, 2003), p.153.
- [88] N.E. Kornienko, In: *Actual problems of solid state physics* (Reports of International scientific conference FTT, Minsk, 2007).
- [89] T.N. Zavarnitskaya, N.N. Mel'nik, V.A. Karavanskii, *JETP Letters* 79(6), 340 (2004) (<https://doi.org/10.1134/1.1759410>).
- [90] M.E. Kornienko, N.L. Sheiko, O.M. Kornienko, T.Yu. Nikolaenko, *Ukr. J. Phys.*, 58(2), 151 (2013) (<https://doi.org/10.15407/ujpe58.02>).
- [91] N.E. Kornienko, A.N. Kirichenko, *Izvestiya vuzov* 59(9), 50 (2016).
- [92] N.E. Kornienko, V.I. Grygoruk, A.N. Kornienko, *Tambov University Reports. Series: Natural and Technical Sciences* 15(3), 953 (2010).
- [93] P. Rai, D.R. Mohapatra, K.S. Hazra, D.S. Misra, Jay Ghatak, P.V. Satyam, *Chem. Phys. Lett.* 455(1-3), 83 (2008) (<https://doi.org/10.1016/j.cplett.2008.02.057>).

Спостереження графіто- і алмазоподібних наноструктур в спектрах раманівського розсіяння природних і синтезованих кристалів MoS₂ з малими добавками вуглецю

¹Київський національний університет імені Тараса Шевченка, Київ, Україна, nikkorn@univ.kiev.ua,
a_naumenko@univ.kiev.ua

²Інститут проблем матеріалознавства імені Францевича НАН України, Київ, Україна, leonid.kulikov.2402@gmail.com

Вперше з використанням раманівської спектроскопії вивчені алмазо- і графітоподібні наноструктури в природному молібденіті і синтезованому монокристалі 2H-MoS₂, а також проведено порівняльне вивчення вуглецевих наноструктур в синтезованих нанокристалітах MoS₂(C) з добавками вуглецю 0,5 і 1,0 мас.%. Детальний чисельний аналіз форми спостережуваних в спектрах D і G смуг при лазерному збудженні $\lambda_L = 632,8$ і 488 нм, включаючи їх розкладання на складові спектральні компоненти, дозволив встановити наявність компонент D(k), G(k), відповідних краям зон Бріллюена, і D(k'), G(k') відповідаючих їх середнім частинам, що свідчить про важливу роль процесів подвоєння розмірів елементарних квазікомірок. Встановлено рекордно низькі частоти D ліній $1284, 1295 - 1312$ см⁻¹ і високі частоти смуг G(k) 1387 і 1402 см⁻¹, які вказують на розміри алмазо- і графітоподібних наноструктур менше 1 нм і звуження їх фононних квазізон. Для надійного розділення близьких коливальних смуг $D \approx G(k)$ використано новий підхід: при зменшенні розмірів і розупорядкуванні наноструктур частоти D смуг зменшуються, а частоти G(k) смуг - зростають. Вперше встановлено значний вплив резонансного випромінювання $632,8$ нм на утворення нанокомпозиту MoS₂+MoO₃, що активує утворення та впорядкування вуглецевих наноструктур. Встановлено підсилення D смуг алмазоподібної наноструктури і впорядкування графітоподібної при зростанні вмісту вуглецю в нанокристалітах MoS₂(C). Розглянуто зміну частот смуг D, G і G(k) при посиленні ступеня розупорядкування алмазо- і графітоподібних структур.

Ключові слова: природні і синтезовані монокристали 2H-MoS₂, нанокристаліти з добавками вуглецю, раманівські спектри, структура D і G смуг, графіто- і алмазоподібні наноструктури.